Supporting Information

A robust new tool for online solution-phase sampling of crystallizations

Andrew J. Kukor,[a] Mason A. Guy, [a] Joel M. Hawkins,*[b] and Jason E. Hein**[a]

[a] Department of Chemistry, The University of British Columbia, Vancouver, BC V6T 1Z1, Canada

[b] Pfizer Global R&D, Groton, Connecticut, 06371, USA

*email for J. H.: joel.m.hawkins@pfizer.com

**email for J.E.H.: jhein@chem.ubc.ca

Table of Contents

1. General Info

a. Chemical Suppliers

(+)-Camphorsulfonic acid was purchased from AK Scientific. Tetrabenazine and tetrabenazine diastereomer were synthesized. *N,N*-diisopropylethylamine and 2-propanol were purchased from Sigma. Sodium iodide and optima-grade ultra-high performance liquid chromatography (UHPLC) solvents were purchased from Fisher. 6,7-dimethoxy-1,2,3,4-tetrahydro-quinoline hydrochloride salt and 3-[(dimethylamino)methyl]-5-methylhexan-2-one oxalate were supplied by Neurocrine Biosciences Inc. All other reagents and solvents were purchased from conventional suppliers and used as received unless otherwise stated. Silica gel was purchased from Silicycle (60 Å, 230 x 400 mesh). RedisepRf gold column was purchased from Fisher Scientific.

b. Equipment Setup

All experiments were performed in Mettler-Toledo EasyMax 102 Advanced Thermostat System glass reactors (100 mL or 250 mL) equipped with Teflon reactor covers, submersible thermocouple, and a magnetic stir bar controlled by the Mettler-Toledo software iControl 6.1. The internal reactor temperature (T_r) was maintained by the EasyMax and measured by a thermocouple placed directly inside the reactor.

Temporal concentration data was obtained using a custom-built automation rig comprised of an EasySampler (with attached filter tip), diluent solvent pump, combined 6-port valve, solenoid valve and pressure sensor module (CombiValve) and an Agilent 1290 Infinity HPLC connected in series. Control of all components except the HPLC was carried out by a custom in-house built control module (DI Box) capable of triggering the EasySampler extension and retraction, pump operation and speed, valve positions, monitoring inline pressure, and sending a signal to trigger the collection of HPLC data. This DI Box controls all components necessary for direct injection of samples from the EasySampler onto the HPLC and is operated by means of a custom-built Python script and graphic user interface. Agilent's Chemstation program was used in conjunction with our DI Box in order to acquire and analyze samples as frequently as the sample run times would allow. Sampling events were controlled via third party software sending a signal at the requested sampling frequency (e.g. every 10 minutes) to our Python script, which would then carry out all of the necessary functions required to obtain the sample and transport it via diluent solvent to the HPLC. A normal sampling sequence with the running Python script looks like:

1. Third party software sends the signal to our Python script that it is time to begin the sampling sequence
2. The EasySampler is extended
3. The pump is started and pre-fills the lines with a specified volume of diluent solvent at a specified flow rate
4. The EasySampler is retracted
5. The 6-port valve position is changed such that the sample loop is now inline with the pump and EasySampler
6. The pump is started and pushes the sample through the lines into the inline sample loop on the 6-port valve
7. The 6-port valve position is changed such that the sample loop is now inline with the HPLC
8. A signal is sent from the DI Box to the HPLC (Chemstation) to begin data collection

9. The pump is started and the lines are washed with a specified volume of diluent solvent
10. The solenoid valve is actuated and an alternate solvent is selected
11. The pump is started and the lines are filled with the alternate solvent (such that extension of the EasySampler introduces 20 µL of this solvent and not diluent into the reaction)
12. The solenoid valve is actuated and returned to the diluent solvent position for the next sampling sequence
13. The third part software waits for a signal from Chemstation that the current HPLC run is over before sending the signal to begin the next run

Mettler-Toledo's iC IR software was used in conjunction with a Mettler-Toledo ReactIR probe for the acquisition of IR data. Mettler-Toledo's iC Vision software was used in conjunction with a Mettler-Toledo EasyViewer probe for the acquisition of turbidity data and crystal images. The setup of the automation rig with all probes in place is shown in **Figure SI 1.**
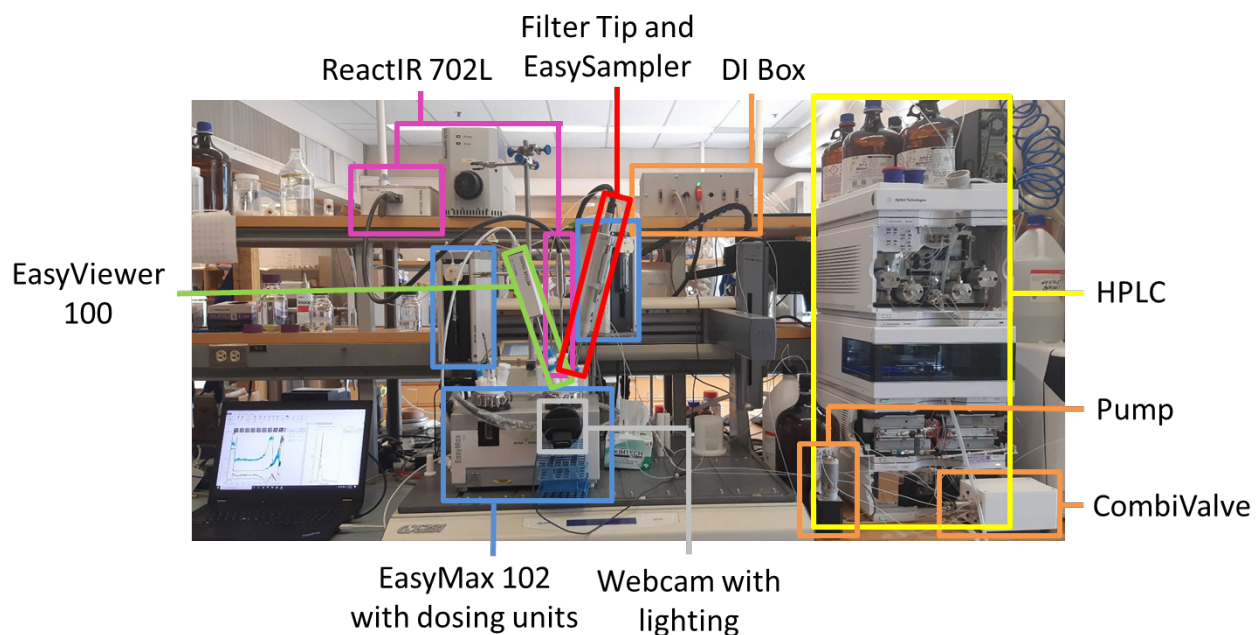
Figure SI 1. Setup of custom-built online HPLC automation rig. Components include: EasyMax 102 with dosing units (blue), EasySampler with attached Filter Tip (red), ReactIR probe and detector (pink), EasyViewer 100 (green), DI Box with pump and CombiValve (orange), and HPLC (yellow). Laptop computer controlling all Mettler-Toledo software is shown on far left. Desktop computer controlling Chemstation, Python script and third party software is out of frame on far right.

c. Analytical Methods

Online HPLC analysis was performed on an Agilent 1290 Infinity HPLC equipped with DAD detector. The collected samples were analyzed using one of the following methods:

General Method: Agilent HPH C18 Column, 2.1 x 50 mm; 2.7 µm
Solvent A = Water; Solvent B = Methanol (0.1 % DIPA v/v)
Flow Rate = 0.450 mL/min
Column Temperature = ambient
Sample Loop Volume = 100 µL
Gradient: A:B 90:10 - initial
AB: 0:100 – 7 min
7.5 min stoptime, no postime

Chiral Method: Daicel IC-3 Chiralpak Column, 2.1 x 150 mm; 3 µm
Solvent A = Water; Solvent B = Methanol (0.1 % DIPA v/v)
Flow Rate = 0.400 mL/min
Column Temperature = 45 °C
Sample Loop Volume = 100 µL
Gradient: A:B 90:10 - initial
A:B 0:100 – 7min
7.5 min stoptime, no postime

Offline HPLC analysis was performed on an Agilent 1290 HPLC equipped with DAD (G4212A) and quadrupole MS (G6140A) detectors. The following method was used to analyze samples:

Agilent Poroshell C18 Column, 2.1 x 50 mm; 1.9 µm
Solvent A = Water; Solvent B = Acetonitrile
Flow Rate = 0.950 mL/min
Column Temperature = 25 °C
Injection Volume = 2.00 µL
Gradient: A:B 95:5 - initial
A:B 70:30 - 3.5 min
AB: 5:95 – 4.5 min
5.5 min stoptime, 1 min postime

NMR spectra were recorded on Bruker NMR spectrometers located within the UBC Department of Chemistry. Data for 1H NMR spectra are listed as follows: chemical shift (δ, ppm), multiplicity, coupling constant (Hz), integration, and are referenced to the residual solvent peak. Abbreviations are as follows: s = singlet, d = doublet, t = triplet, q = quartet, p = pentet, m = multiplet. $^{13}C\{^1H\}$ NMR spectra are listed in terms of chemical shift (δ, ppm). In situ FT-IR monitoring was conducted with a Mettler-Toledo ReactIR 702L equipped with a SiComp (silicon) ATR probe connected via an AgX (silver halide) 6.3 mm x 1.5 m fiber optic cable. Spectra were recorded over 3000 cm^{-1} to 650 cm^{-1} at 4 cm^{-1} resolution with 1x gain.
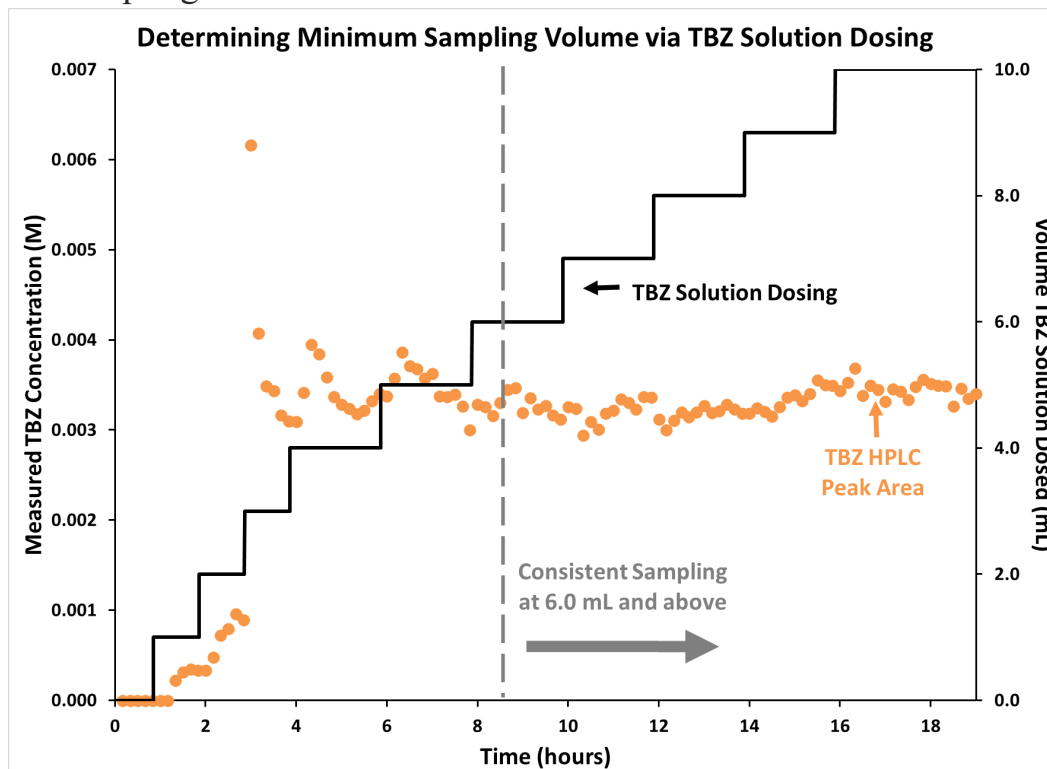
2. Filter Tip

a. Filter Tip Specifications

Figure SI 2. Left to right: Image of bushing, screw and filter tip unassembled

      The filter tip is a hollow half-cylinder composed of sintered steel with 10 μm pores measuring 25.3 mm long and 12.7 mm wide (outer diameter). The inner diameter is 9.47 mm, which fits snugly on the outer diameter of the replaceable EasySampler sleeve (which measures 9.49 mm). Slight variations in EasySampler sleeve outer diameters resulted in some sleeves not fitting within the filter. The filter itself was purchased from Cole-Palmer and is the replacement filter for the Idex A-550 Stainless Steel Bottom-of-the-Bottle™ Assembly. A 3.0 mm hole was drilled in the end of the filter to allow for a small screw to be inserted through this opening. A hole was drilled in the end of the actuating EasySampler head and a brass bushing threaded to match the screw was pressure-fit into this hole. This allowed for attachment of the filter tip to the EasySampler head with the screw such that the entire assembly moves when the EasySampler head is extended or retracted.

b. Minimum Sampling Volume - Results and Discussion

Figure SI 3. Dosing homogeneous 0.0035 M TBZ solution in IPA in 1.0 mL increments into a 20.0 mL scintillation vial to determine the minimum volume required for accurate, reproducible sampling.

Before using the filter tip to monitor any processes, it was necessary to determine the minimum filter submersion depth required for accurate and reproducible sampling of solution concentrations. To this end, the filter tip was inserted into a 20.0 mL scintillation vial while samples were acquired in 10 minute intervals. 0.0035 M TBZ solution in IPA was dosed in 1.0 mL increments on an hourly basis for the first 4.0 mL, with little entering the filter when less than 3.0 mL of solution was present and the tip of the filter simply actuating in and out of these minimal volumes. The observed HPLC peak areas increased dramatically upon addition of the 3rd mL of TBZ solution, far exceeding the actual concentration of 0.0035 M. This is consistent with TBZ residue building up inside the filter tip as it entered and exited the solution when less than 3.0 mL was present (being only partially submerged). We propose that the porosity of the filter allows for solution to be wicked up through the filter during partial submersion. Therefore, the residue left behind during previous extensions/retractions would later be dissolved upon further solution dosing, resulting in larger peak areas. These peak areas then decreased to the true solution concentration as the residue was completely dissolved and only the 0.0035 M solution remained – hence the oscillatory nature of the peak areas increasing as residue was submerged, and decreasing as it was fully dissolved. Solution was dosed on a bihourly basis for the last 6 mL, and oscillating behaviour was determined to be minimal after a total of 6.0 mL of solution had been added. This suggests submersion to at least a depth of 6.0 mL in a 20.0 mL scintillation vial (or to a depth of 14.0 mm when extended) is necessary to prevent this solute residue buildup and dissolution from occurring as the EasySampler is extended into and out of the solution, and that precise concentration data can be obtained under these conditions (**Figure SI 4**).
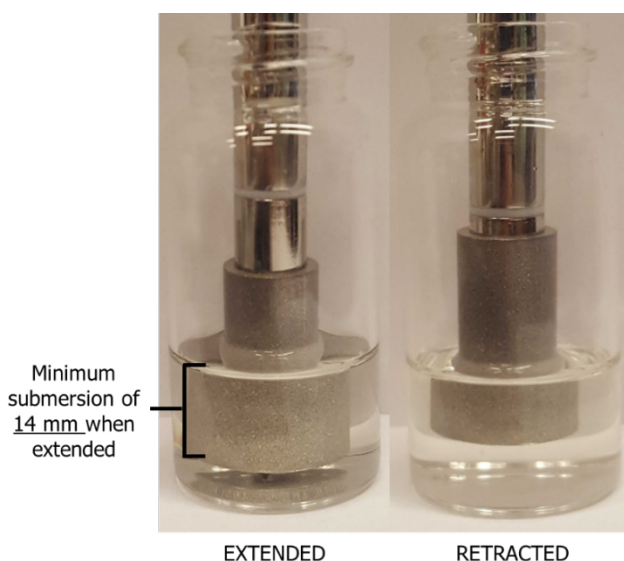
Figure SI 4. Image of EasySampler with filter tip attached, illustrating minimum volume (6.0 mL in a 20.0 mL scintillation vial) and minimum submersion depth (14.0 mm when extended) required for reproducible sampling.

The oscillatory pattern in the concentration data was completely absent after 8.0 mL of solution had been dosed, and a slight increase in concentration was observed after 9.0 mL had been added. This indicates that at least 8.0 mL of solution (or submersed to a depth of 18.0 mm) may be required for the filter to be constantly wet, therefore preventing residue from building up inside as solution evaporates.

The observed increase in concentration upon reaching 9.0 mL (or submersed to a depth of 20.0 mm) may be due to an increased filling efficiency of the filter tip interstitial space upon larger submersion depths – see SI section **7** for further discussion on this point. Ultimately, the return of the concentration data to roughly the same location after each dosing event beyond 3.0 mL suggests that the filter tip is highly reproducible at any given submersion depth. However, changing submersion depths may change the filter filling efficiency and thus result in different amounts of solute being sampled. Furthermore, these numbers may differ as the composition and temperature of the solvent change as these may affect how well solvent is wicked up the filter at low submersion depths, or how difficult it is for solvent to pass through the 10 µm pores of the filter if the viscosity is especially high.

3. Synthetic Procedures

a. Tetrabenazine (TBZ)
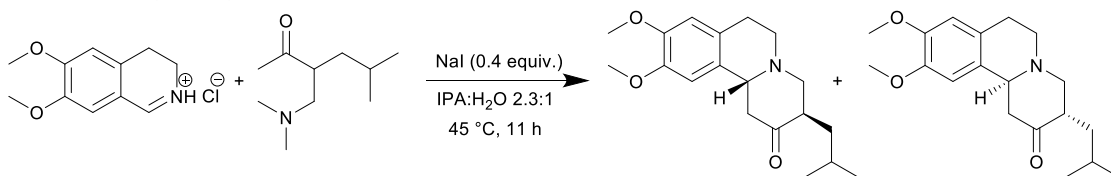
To a 100 mL EasyMax flask equipped with a stir bar were added isopropyl alcohol (IPA; 20.4 mL), water (8.8 mL), 3-[(dimethylamino)methyl]-5-methylhexan-2-one (5.48 g, 32.00 mmol, 1.25 equiv.), 6,7-dimethoxy-1,2,3,4-tetrahydro-quinoline hydrochloride salt (5.83 g, 25.60 mmol, 1.00 equiv.), and NaI (1.53 g, 10.24 mmol, 0.40 equiv.). The mixture was stirred vigorously for 11 hours at 45 °C. 12 mL of water was then added to the mixture at 0.1 mL/min, after which the mixture was cooled to 5°C at 0.1 K/min. The mixture was filtered to afford tetrabenazine (4.58 g, 56.3%) as a white crystal. ^{1}H NMR (400 MHz, CDCl$_3$) δ 6.62 (s, 1H), 6.55 (s, 1H), 3.86 (s, 3H), 3.83 (s, 3H), 3.51 (dd, J = 11.8, 2.9 Hz, 1H), 3.29 (dd, J = 11.5, 6.3 Hz, 1H), 3.19 – 3.05 (m, 2H), 2.90 (dd, J = 13.6, 3.1 Hz, 1H), 2.81 – 2.67 (m, 2H), 2.64 – 2.49 (m, 2H), 2.36 (t, J = 11.6 Hz, 1H), 1.80 (ddd, J = 13.9, 8.5, 5.5 Hz, 1H), 1.66 (ddt, J = 12.9, 8.5, 6.5 Hz, 1H), 1.04 (ddd, J = 13.6, 7.4, 5.8 Hz, 1H), 0.92 (appt dd, J = 6.6, 4.7 Hz, 6H); ^{13}C NMR (100 MHz, CDCl$_3$) δ 210.1, 147.9, 147.6, 128.5, 126.1, 111.5, 107.9, 62.5, 61.5, 56.1, 56.0, 50.7, 47.6, 47.5, 35.1, 29.4, 25.5, 23.3, 22.2; MS ESI$^+$ (calc. for C$_{19}$H$_{27}$NO$_3$, 317.20): m/z = 318.2 [M+H]$^+$.

b. TBZ Diastereomer
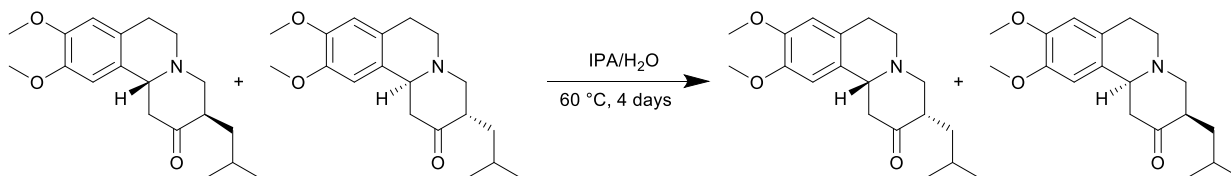
To a 100 mL EasyMax flask equipped with a stir bar was added crude, unfiltered reaction mixture from a TBZ synthesis reaction. The mixture was stirred vigorously at 60 °C for 4 days to produce the diastereomer, then cooled to 5 °C at 0.1 K/min and filtered to separate out the solid TBZ. The filtrate containing TBZ and the TBZ diastereomer then had solvent removed in vacuo and was dissolved in 30 mL DCM. Silica gel (5 g) was then added, and solvent again removed in vacuo. The dry-loaded solids were then purified via flash column chromatography (0-70% EtOAc in Hexanes) using a RediSepRf gold column (24 g) to afford 30 mg of TBZ diastereomer (30 mg, 0.4%)as an off-white solid. ^{1}H NMR (400 MHz, CDCl$_3$) δ 6.62 (s, 1H), 6.56 (s, 1H), 3.86 (s, 3H), 3.83 (s, 3H), 3.44 (br d, J = 11.5 Hz, 1H), 3.19 – 3.08 (m, 1H), 3.07 – 2.93 (m, 2H), 2.82 (ddd, J = 14.2, 3.3, 1.5 Hz, 1H), 2.72 (dd, J = 11.6, 4.0 Hz, 1H), 2.68 – 2.59 (m, 2H), 2.58 – 2.49 (m, 2H), 1.85 – 1.73 (m, 1H), 1.60 – 1.46 (m, 2 H), 0.93 (d, J = 6.2 Hz, 3H), 0.88 (d, J = 6.3 Hz, 3H); ^{13}C NMR (100 MHz, CDCl$_3$) δ 212.6, 147.7, 147.7, 128.9, 126.6, 111.4, 107.8, 62.2, 59.8, 56.1, 56.0, 51.8, 49.2, 45.4, 40.7, 29.4, 25.9, 22.8, 22.4; MS ESI$^+$ (calc. for C$_{19}$H$_{27}$NO$_3$, 317.20): m/z = 318.2 [M+H]$^+$.

Note: The diastereomer is proposed to be in equilibrium with TBZ in a ratio of ~1:10 in polar protic solution due to the epimerization at atom 17, resulting in diastereomer production during all TBZ synthesis reactions but making diastereomer isolation extremely challenging. Heat was used to promote this epimerization, followed by cooling to crystallize out most of the TBZ (see **Figure SI 13** for chromatograms of solution before and after). However, exposure to acidic media or polar protic solvent seemed to convert the diastereomer back into TBZ, resulting in the extremely low yield of 30 mg after column chromatography due to the acidic nature of silica gel. NMR analysis (via HSQC comparison between the diastereomer and TBZ) was consisted with the expected spectrum for the diastereomer.

c. (+)-TBZ·(+)-CSA Salt

Synthesis was followed as outlined by Yao et al.[1] for PXRD comparison with classical resolution solid phase.

4. Calibration Curves

a.   Experimental Data
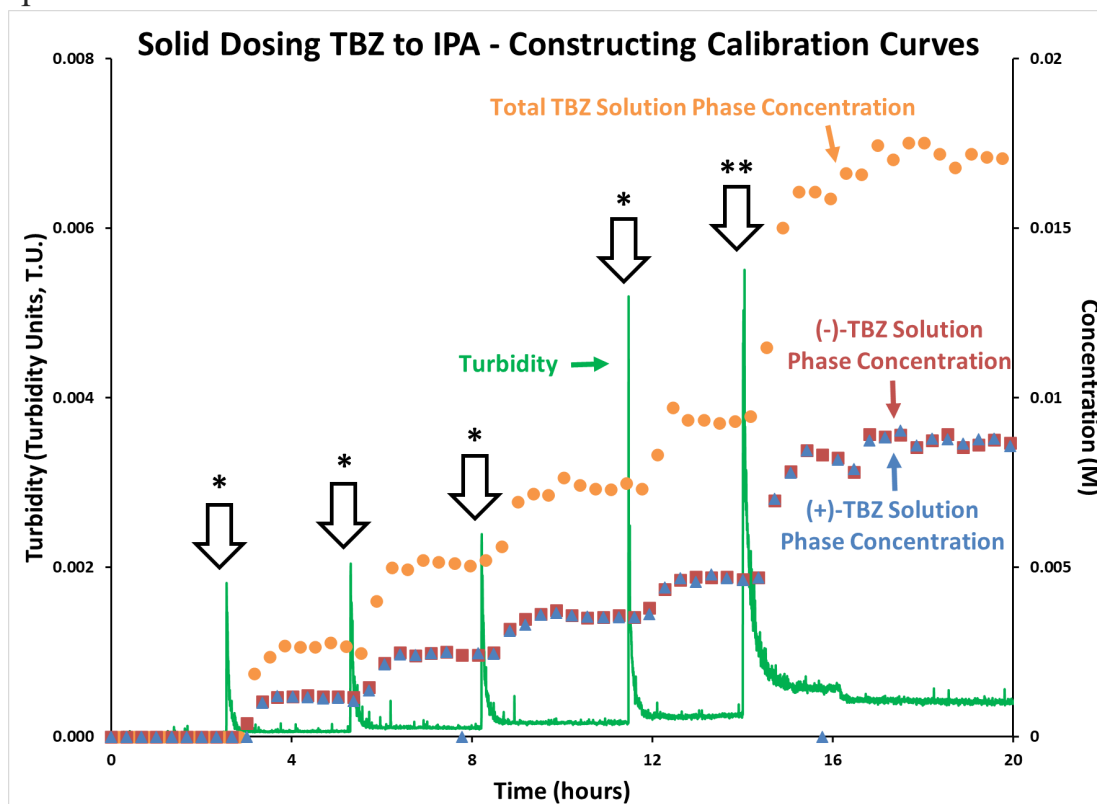
Figure SI 5. Dosing solid TBZ (* = 30 mg, ** = 100 mg) into 40 mL of IPA at 10 °C to obtain calibration curves for TBZ on chiral (IC-3) and achiral (HPH C18) columns

       Data was obtained as outlined below in Experimental Procedures a. Calibration Curves. Peak areas from the chiral (IC-3) and achiral (HPH C18) columns from the plateaus after each dosing event were averaged and plotted against the calculated solution concentration to construct **Figures SI 6** and **7**. Given

the R^2 values of 0.9993 and 0.9999 for the achiral and chiral plots respectively, it can be concluded that sampling TBZ/IPA solutions with our filter tip shows a linear correlation between peak area and analyte solution phase concentration. As such, these figures were applied to each experiment in this paper to convert peak areas into solution phase concentrations.

b. Achiral Calibration Curve

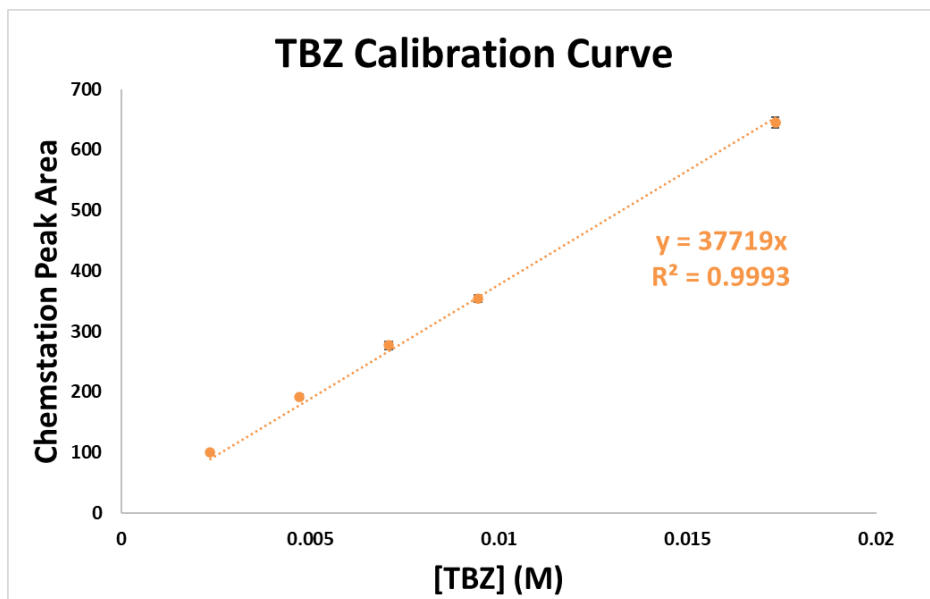
Figure SI 6. TBZ calibration curve for achiral (HPH C18) column (data from **Figure SI 5**).
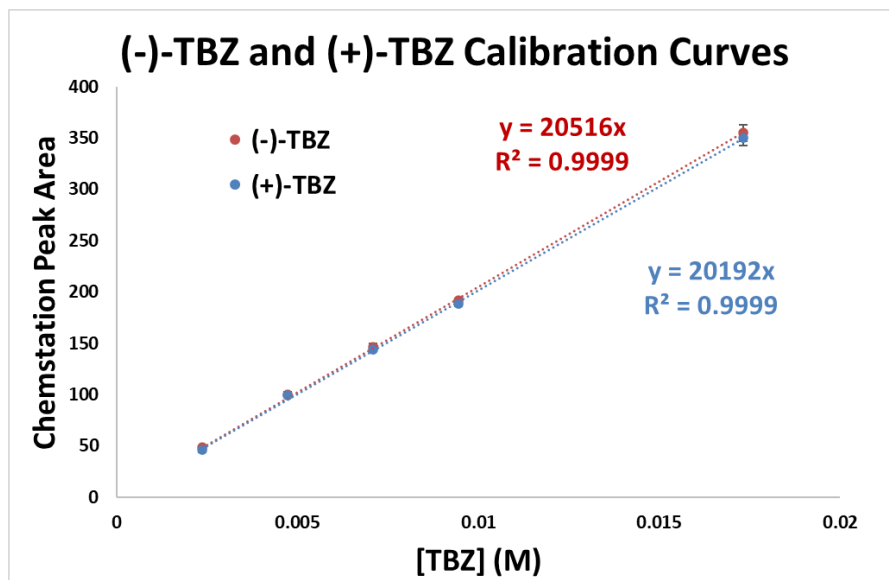
c. Chiral Calibration Curves

Figure SI 7. (-)-TBZ and (+)-TBZ calibration curves for achiral (IC-3) column (data from **Figure SI 5**).

5. Experimental Procedures

a. Calibration Curves (Figures SI 5-7)

40 mL of IPA stirring at 200 rpm at 10 °C was automatically sampled every 10 minutes by the EasySampler/filter tip assembly while monitoring turbidity via the EasyViewer. HPLC analysis was performed using alternating chiral (IC-3) and achiral (HPH C18) columns. After sampling pure IPA for 2 hours, solid TBZ (30 mg, 0.095 mmol) was dosed in via the top of the reactor and was observed to dissolved via turbidity returning to baseline. This was mirrored in the HPLC peak areas increasing to a plateau, as expected. Subsequent solid TBZ dosing was performed at roughly 5 hours (30 mg, 0.095 mmol), 8 hours (30 mg, 0.095 mmol), 12 hours (30 mg, 0.095 mmol), and 14 hours (100 mg, 0.315 mmol). Upon each dosing event, the solution became turbid but returned to homogeneous as evidenced by the turbidity spikes returning to baseline.

b. Solid Dosing (Figure 4)

40 mL of IPA stirring at 200 rpm at 10 °C was automatically sampled every 10 minutes by the EasySampler/filter tip assembly while monitoring turbidity via the EasyViewer. HPLC analysis was performed using an HPH C18 column. After sampling pure IPA for 2.5 hours, solid TBZ (100 mg, 0.315 mmol) was dosed in via the top of the reactor and was observed to dissolved via turbidity returning to baseline. This was mirrored in the HPLC peak areas increasing to a plateau, as expected. Subsequent solid TBZ dosing was performed at roughly 6 hours (100 mg, 0.315 mmol), 7.5 hours (100 mg, 0.315 mmol), 10 hours (200 mg, 0.630 mmol), and 13.5 hours (200 mg, 0.630 mmol). Following the dosing events at 6 and 7.5 hours the solution became turbid but returned to homogeneous as evidenced by the turbidity spikes returning to baseline. Following the dosing event at 10 hours the solution became saturated as evidenced by the large increase in turbidity that did not decrease as before, and by the minimal increase in TBZ solution phase concentration from the previous dose. The final dosing event therefore did not change the TBZ solution phase concentration as the solution was already saturated, instead only further increasing the turbidity.

c. IPA Dosing (Figure 5 and Figure SI 8)

TBZ (400 mg, 1.26 mmol) was added to 55 mL of 1:1 IPA:water (v/v) at 5 °C to produce a 0.023 M TBZ slurry. While stirring at 200 rpm, the slurry was sampled every 10 minutes by the EasySampler/filter tip assembly and monitored turbidity (via EasyViewer) and IR (via ReactIR). HPLC analysis was performed using an HPH C18 column. After sampling the slurry for 30 minutes, 30 mL of IPA was dosed in at 0.1 mL/min, and then solution was sampled for another 30 minutes afterwards. The slurry fully dissolved during the IPA dosing as evidenced by the turbidity reaching zero and the solution phase concentration reaching a maximum value. Continued dosing beyond the analyte dissolution resulted in dilution as seen in the decreasing TBZ solution phase concentration, which stopped decreasing after dosing ceased.

d. Water Dosing (Figure 6)

TBZ (1.50 g, 4.73 mmol) was added to 100 mL of IPA at 25 °C to produce a homogeneous 0.0473 M solution. Stirring at 500 rpm, the solution was sampled every 10 minutes by the EasySampler/filter tip assembly. HPLC analysis was performed using an HPH C18 column. After sampling for 2.5 hours, 80 mL of water was dosed in at 0.2 mL/min to dilute the solution and drive nucleation. This dilution can be seen in the linearly decreasing concentration of TBZ. As nucleation did not yet occur, the solution was cooled to 12 °C at the 5 hour mark and then to 10 °C at the 7 hour mark to further lower the solubility. Nucleation was observed at 7.5 hours, evidenced by a sudden decrease in concentration. The amount of TBZ in solution (calculated from the concentrations and volumes) can be seen to remain relatively constant (as expected) until nucleation occurs, highlighting the accuracy of the concentration data.

e. Water Dosing Repeat with IR and Turbidity (Figure SI 9)

TBZ (635 mg, 2.00 mmol) was dissolved in 42.5 mL of 10:9 IPA:water (v/v) at 23 °C while stirring at 500 rpm (**Figure SI 9**). The solution was sampled every 10 minutes by the EasySampler/filter tip assembly while monitoring turbidity via EasyViewer and IR via ReactIR. HPLC analysis was performed using an HPH C18 column. After sampling the solution for 2 hours, 56.4 mL of water was dosed in at 0.1 mL/min, and then the solution was sampled for another 2 hours afterwards. The solution was first diluted as evidenced by the linearly decreasing TBZ solution concentration. Continued dosing of antisolvent decreased the solubility of TBZ in the solution and resulted in eventual nucleation just after 8 hours, as evidenced by an increase in turbidity and precipitous decrease in TBZ solution concentration beyond the previous decreasing trend. Turbidity spikes were observed prior to nucleation at around 6 hours but the lack of change in the solution phase concentration, combined with EasyViewer images of large particles during this regime, suggests that this was due to localized crystallization events as the solution became supersaturated and was not reflective of total solution nucleation.

f. Heating and Cooling (Figure 7)

TBZ (1.52 g, 4.79 mmol) was added to 200 mL of 1:1 IPA:water (v/v) at 5 °C to produce a 0.0239 M TBZ slurry. While stirring at 500 rpm, the slurry was sampled every 10 minutes by the EasySampler/filter tip assembly while monitoring turbidity via EasyViewer. HPLC analysis was performed using an HPH C18 column. After sampling the slurry for 1 hour, the slurry was heated to 34 °C at 0.1 K/min. The solution was then cooled to 5 °C at 0.2 K/min and sampled for another 3 hours. Initially, increasing the temperature from 5 °C increased the solubility of TBZ in the solution and therefore dissolving the solid phase, as evidenced by the increasing TBZ solution concentrations. Full dissolution was reached at approximately 32 °C, after which point the TBZ solution concentration plateaued. Further heating to 34 °C had no effect on the solution concentration as the TBZ was already fully dissolved. Nucleation was observed after cooling to approximately 14 °C, as evidenced by a sudden decrease in TBZ solution concentration and an increase in turbidity.

g. Heating and Cooling with Diastereomer Impurity (Figure 8)

Prior to the experiment, TBZ was dissolved in IPA and heated to 60 °C for 24 hours while stirring to convert some TBZ into its diastereomer. The solution was then cooled and filtered to obtain TBZ with significant diastereomer impurity. This impure TBZ was then used to prepare 40 mL of 0.23 M TBZ/diastereomer slurry (2.9 g, 9.2 mmol) in IPA stirring at 300 rpm at 5 °C. This slurry was sampled every 10 minutes by the EasySampler/filter tip assembly while monitoring turbidity via EasyViewer. HPLC analysis was performed using an HPH C18 column. After sampling the slurry for 2 hours, the slurry was rapidly heated to 65 °C. This increased the solubility of TBZ in the solution, therefore increasing the TBZ solution phase concentration. The turbidity decreasing to zero is evidence of the solid phase completely dissolving during this time. The 65 °C homogeneous solution was then sampled for 5 hours, then cooled rapidly back to 5 °C. This rapid cooling resulted in the solid phase reforming, as evidenced by the sudden decrease in TBZ solution phase concentrations and the sudden increase in turbidity.

h. Classical Resolution (Figures 9-10, and Figures SI 10, 17 and 18)

100 mL of 1:1 IPA:water (v/v) stirring at 300 rpm at 10 °C was sampled every 10 minutes by the EasySampler/filter tip assembly while monitoring turbidity via EasyViewer. HPLC analysis was performed using alternating chiral (IC-3) and achiral (HPH C18) columns. After sampling the solution for 1 hour, TBZ (15.87 g, 50 mmol) was added to create a 0.5 M slurry. The slurry was sampled for 2 hours, then 0.5 mL was sampled manually using an autopipette and modified pipette tip. After manually sampling, 5.0 mL of 1.0 M (+)-CSA solution (5 mmol, 0.1 equiv.) in 1:1 IPA:water (v/v) was rapidly dosed into the TBZ slurry. 2 hours after this first (+)-CSA dose, a sample was again obtained manually, after which another 5.0 mL of 1.0 M (+)-CSA solution (5 mmol, 0.1 equiv.) was dosed into the slurry. This process was repeated 2 more times. After the 4th (+)-CSA solution dose, the slurry was sampled for 2 hours, then the EasySampler sampling frequency was reduced to every 30 minutes overnight.

11 hours later, sampling frequency was returned to every 10 minutes, but a data conversion error resulted in sampling stopping for 1.5 hours. Sampling every 10 minutes then resumed, and the slurry was sampled for 2 hours. Manual sampling then occurred, followed by dosing another 5.0 mL of 1.0 M (+)-CSA solution (5 mmol, 0.1 equiv.) and subsequent sampling of the slurry for 2 hours. This was repeated 4 more times until (+)-CSA solution had now been dosed a total of 9 times into the solution (with the total (+)-CSA added being 45 mmol, or 0.90 equiv.). EasySampler sampling frequency was again reduced to every 30 minutes overnight.

11 hours later, sampling frequency was returned to every 10 minutes and the slurry was sampled for 2 hours. Manual sampling again occurred, followed by dosing 1.0 mL of 1.0 M (+)-CSA solution (1 mmol, 0.02 equiv.) and waiting 2 hours. This process was repeated 3 more times for a total of 49 mmol of (+)-CSA (0.98 equiv.). The experiment was then ended as the data files had unfortunately grown too large to accommodate a final dosing event.

All manual samples were immediately deposited into a centrifuge tube with 0.45 mm Nylon filter and centrifuged at 10 °C and 9000 rpm for 10 minutes. The impacted solids were subsequently dissolved in methanol, and then analyzed via chiral (IC-3) HPLC along with the filtrate to determine the e.e.'s of the solid and liquid phases of the resolution, respectively.

6. Infrared Data from Experiments

a. IPA Dosing
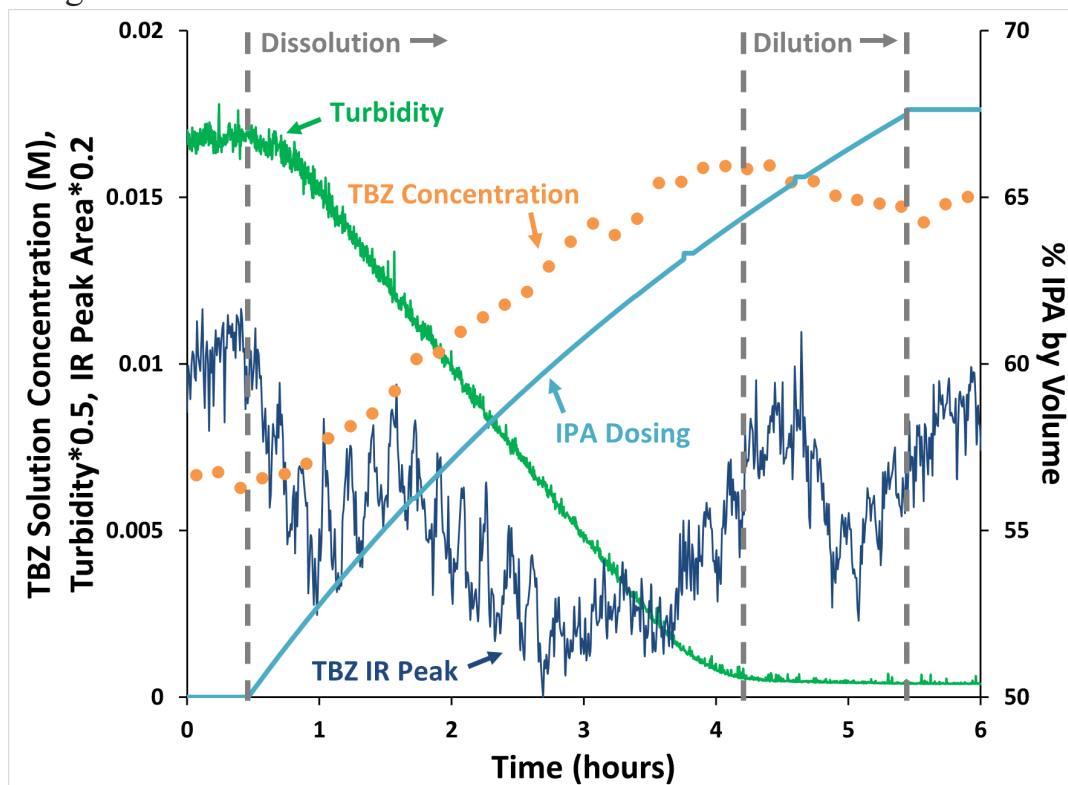
Figure SI 8. IPA dosing into 1:1 IPA:water (v/v) heterogeneous TBZ solution (same as **Figure 5**), with TBZ IR peak overlaid on top of turbidity, dosing and concentration data to illustrate the poor correlation. Turbidity values and IR peak areas were multiplied by constants (0.5 and 0.2 respectively) to be plotted on the same axis as concentration.

The IR trends observed during the IPA dosing experiment clearly do not follow the TBZ solution phase concentration data obtained with the filter tip. This is due to the changing solvent composition: the TBZ IR peak integrated at 1520 cm^{-1} is on the shoulder of the significantly larger solvent peaks. As such, changing solvent composition compromises the utility of subtracting the initial background solvent signals acquired before analyte was added and makes analysis of the data nontrivial. While advanced chemometric tools may be able to deconvolute the IR data, **Figure SI 8** shows the author's best attempts at using solvent subtraction and peak area integration to pick out the TBZ trend over time. Clearly, it is much more straightforward to use the filter tip and HPLC data to obtain concentration information in scenarios such as this.

b. Water Dosing
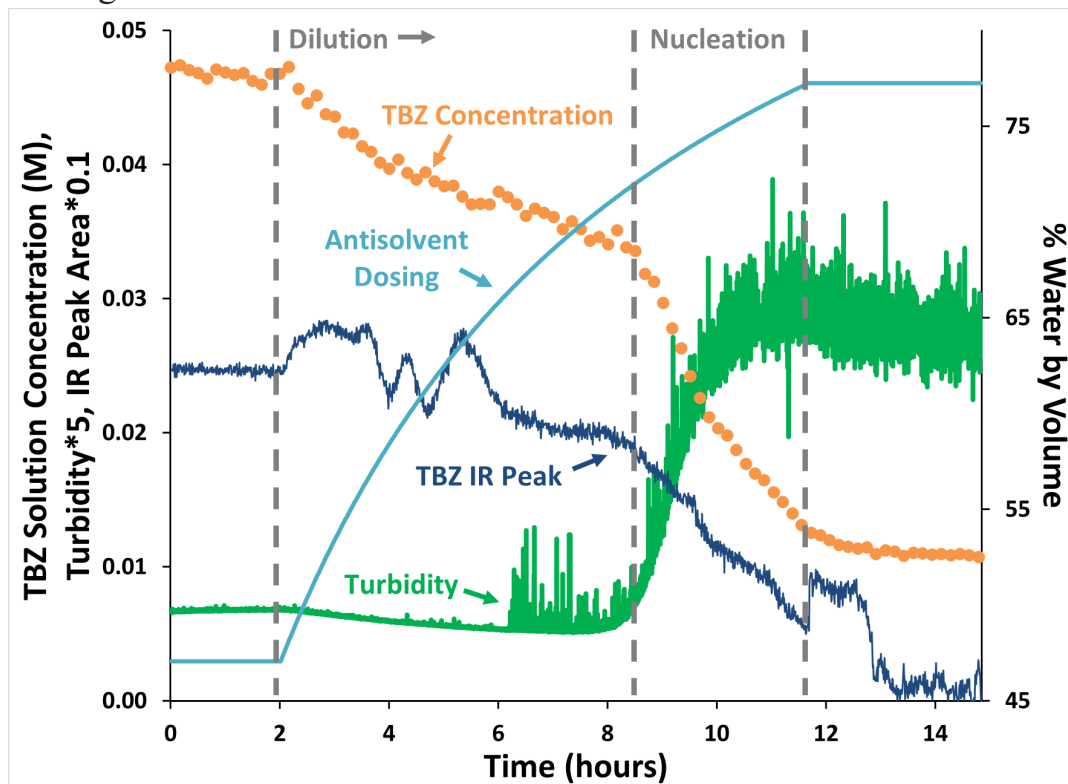
Figure SI 9. Water (antisolvent) dosing into 42.5 mL of 1:1 IPA:water (v/v) homogeneous 0.047 M TBZ solution. The TBZ IR peak is overlaid on top of turbidity, dosing and concentration data to illustrate their moderate correlation.

The water dosing experiment was repeated with the use of an EasyViewer and ReactIR to test the effectiveness of monitoring with IR (and supplemented with turbidity information). Unlike IPA dosing, the water dosing showed a significantly clearer IR trend: upon nucleation, the trend can clearly be seen to decrease. However, the changing solvent composition again makes data treatment extremely difficult. Significant noise can be seen from approximately 2-6 hours and again around 12 hours. This does not match any trends in either the TBZ solution concentration data nor the turbidity data, suggesting that this is due to changes in peak shape as solvent composition changes and integration of the TBZ peak is made different. As such, this graph also highlights the ease of using the filter tip and HPLC to obtain solution phase concentration information in a complex system.

c. CSA Dosing
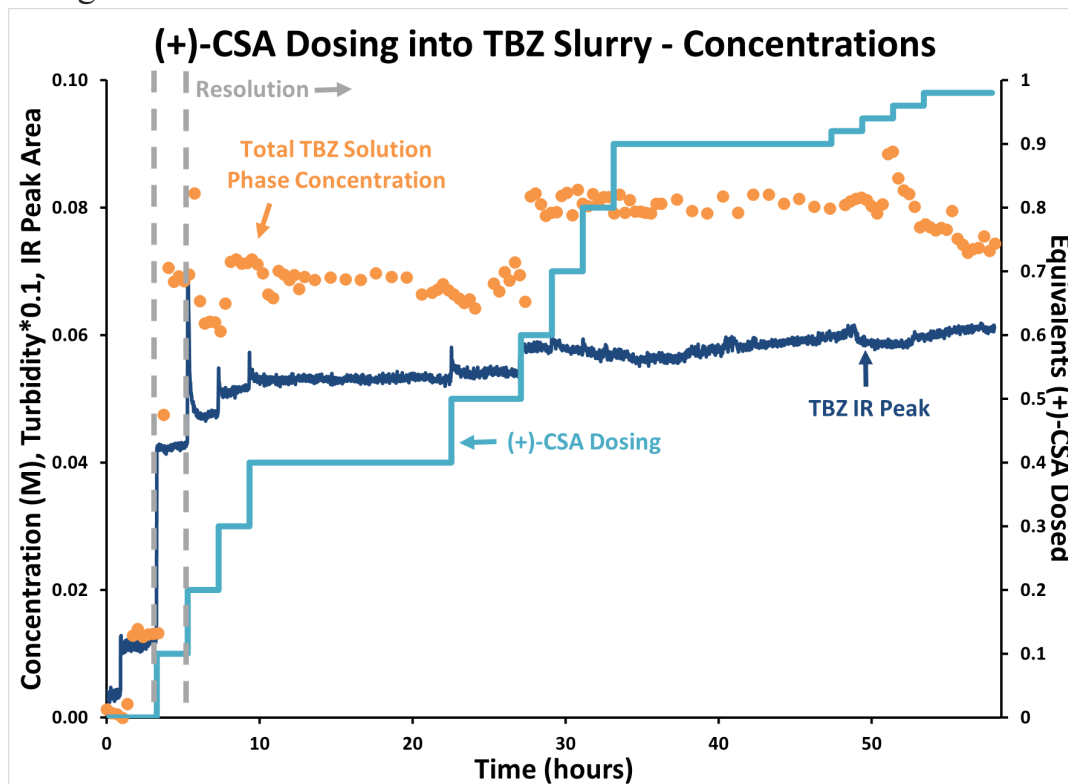
Figure SI 10. (+)-CSA dosing into TBZ-saturated slurry in 1:1 IPA:water (v/v) with IR trend overlaid.

Without changing solvent composition, IR proved to be as effective as HPLC at monitoring total TBZ solution concentration with the IR trend in **Figure SI 10** closely matching that obtained with the filter tip for solution concentration. Nonetheless, no chiral information is available via IR for this or similar systems and this data is therefore extremely limited for such purposes as chiral resolution monitoring.

7. Filter Tip Limitations: Filling Efficiency

a. Submersion Depth
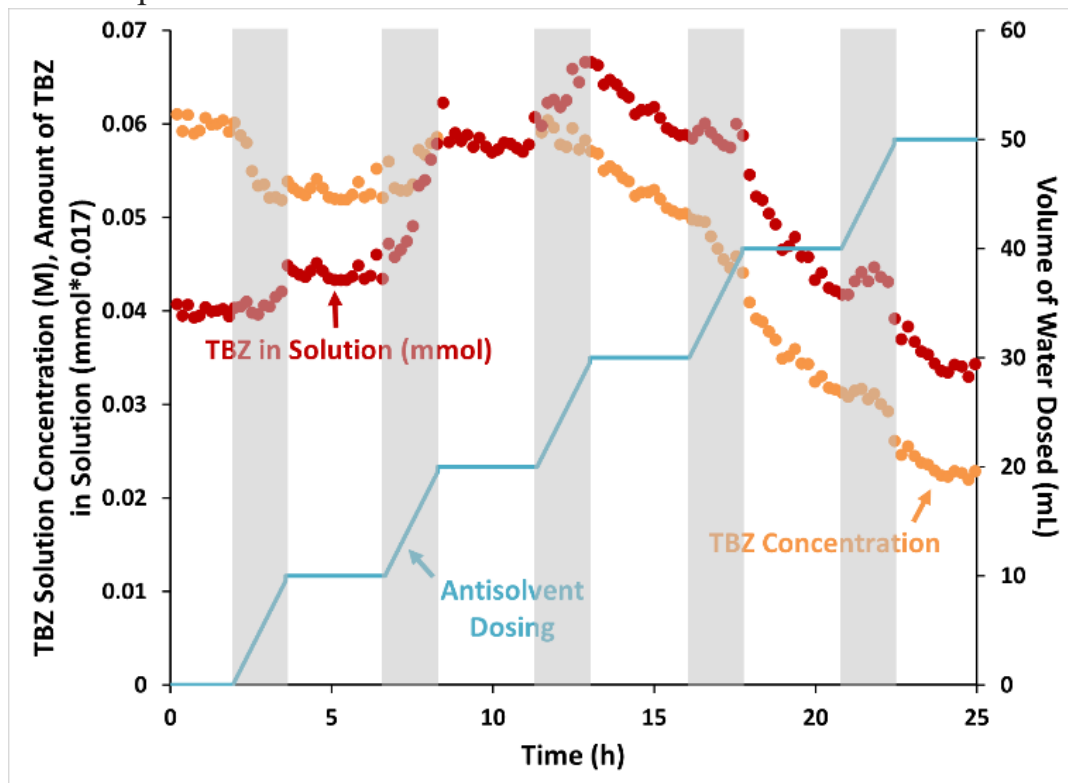
Figure SI 11. Water (antisolvent) dosing into 1:1 IPA:water (v/v) homogeneous 0.06 M TBZ solution at 25 °C with pausing (white) between dosing events (grey) to determine the effect of changing submersion depth on filter tip filling efficiency. Nucleation can be seen after 13 hours, driving down concentration when no dosing was occurring.

The initial minimum sampling volume test (**Figure SI 3**) suggested that sampling was highly reproducible at submersion depths beyond 14.0 mm (when the EasySampler is extended). However, later results indicated that partial and complete submersion of the filter may give different analyte concentrations (putting the accuracy into question). To explicitly demonstrate this, the water dosing experiment was repeated starting with the filter only partially submerged (**Figure SI 11**). Antisolvent (water) was dosed in increments with intentional pauses where no dosing occurred to determine the effect of changing reactor volume (and thus submersion depth) over time. While the first dosing event can be seen to lower the TBZ solution concentration as expected, the concentration appears to increase after the second dosing event. This is not possible if the solution is only being diluted, therefore suggesting that more sample may be entering the filter tip at this higher reactor volume than was previously. This would then result in an apparently larger solution concentration if a greater amount of sample enters the 20 μL sample pocket and is delivered to the HPLC for analysis. No change in solution concentration was observed in the pausing between the first and second dosing events, further suggesting that it was the act of dosing that was responsible for changing the filter filling efficiency (and not something related to sampling events themselves, otherwise changes would still occur during the "pause").

The next dosing event showed no decrease in solution concentration despite further dilution occurring, again suggesting that the filter filling efficiency was improving as the reactor volume further increased. However, nucleation began at the end of this dosing event, resulting in a decrease in solution concentration during the subsequent pause from 13 to 16 hours. The next dosing event seems to have again increased filter filling efficiency at the beginning, as despite dilution occurring the solution concentration appeared constant for the first hour. Nucleation then occurred again and continued into the next wait, decreasing the observed solution concentration of TBZ. The final water dosing showed identical behaviour, where the expected decrease in concentration was not observed immediately and only occurred after some time.

Due to this evidence of changing submersion depth affecting the filter filling efficiency, it is therefore recommended that if the reactor volume is to be changed during an experiment (e.g. during solvent or antisolvent dosing) that the filter tip be entirely submerged in the solution at all times. **Figure SI 3** supports the precision of the concentration data obtained with the filter tip even at partial submersion, but the data in **Figure SI 11** clearly indicates that changing the submersion depth will affect the acquired concentration data. This changing filling efficiency is proposed to be due to the physical constraints of the filter tip herein presented. As the filter is porous, it is likely that an only partially submerged filter can pull air through the top of the filter. Furthermore, the internal diameter of the filter seals on the outer diameter of the EasySampler simply through metal-on-metal tolerance. As such, this seal is likely not perfect and may further be contributing to different filter filling efficiencies when the probe is partially vs. fully submerged.

b. Viscosity

In addition to submersion depth changing throughout the water dosing experiment, the solvent composition also changed. This may also be a contributing factor to changing filter filling efficiency as more viscous solutions would be expected to be more difficult to pull through the filter (and thus risk more air being pulled through the top if the filter is not fully submersed). During the repeated water dosing experiment (**Figure SI 11**), the solvent composition changed from 53% to 23 % IPA in water (v/v), therefore decreasing from roughly 3.1 cP to 2.2 cP, or -0.9 cP overall.[2] Conversely, during the IPA dosing experiment (**Figure 5**) the solvent composition changed from 50% to 68% IPA in water (v/v) or from roughly 3.1 cP to 2.9 cP at 25 °C, or only -0.2 cP overall (becoming slightly less viscous).[2] Thus, the water dosing experiment clearly experienced a significantly less viscous solution at the end, which may explain why such different filter filling efficiencies were observed (in addition to the changing submersion depth).

c. High Solids Loading

During the (+)-CSA dosing experiment, a slight lag was observed between the immediate changes observed in the turbidity data upon dosing and the TBZ solution phase data. Given the extremely high solids loading used in this experiment, we propose that this lag was due to solids coating the surface of the filter. The quality of the data obtained suggests that the filter was not completely fouled by these solids and that the dynamic self-flushing behaviour was successful at keeping the filter pores unclogged. However, the high solids loading may have resulted in crystals accreting to the filter and increasing the difficulty of pulling solution through the filter. This would have reduced the efficiency with which the filter is flushed with each extension and retraction cycle, requiring multiple sampling cycles for the inside

of the filter to reflect the solution composition and therefore resulting in the observed lag in the time course data.

d. Temperature and Cavitation

The automated sampling sequence we used involved pre-filling the EasySampler lines and sample pocket with solvent. Thus, when the EasySampler head is extended, a small amount of this pure solvent is present in the filter as it is extended. At higher temperatures, we propose that this increases the risk of this solvent cavitating in the filter and therefore pulling in less solution to be sampled. Since cavitation is a stochastic phenomenon, this would reduce the precision of samples obtained at higher temperatures. Increased noise in the concentration data obtained at elevated temperatures (mild at 30 °C (**Figure 7**) and moderate at 65 °C (**Figure 8**) during their respective heating/cooling experiments) fits this expected behaviour, supporting this hypothesis.

8. Supporting Images

a. HPLC Chromatograms
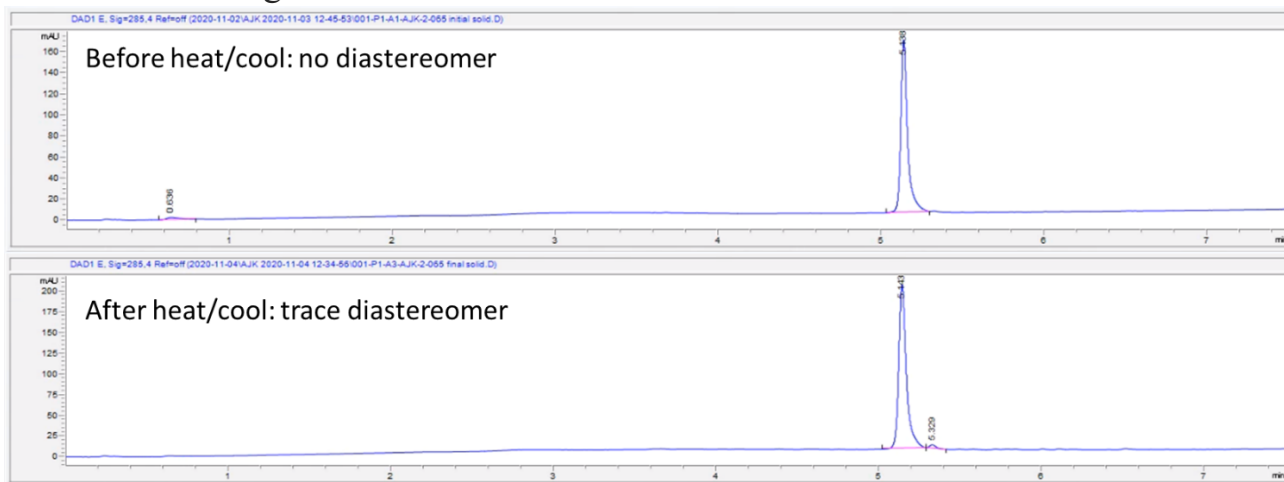
Figure SI 12. HPLC traces (285 nm) of solid phases isolated before (above) and after (below) rapid heating and cooling experiment. TBZ is visible at 5.1 minutes with little/no diastereomer at 5.3 minutes both before and after rapid heating and cooling, indicating the diastereomer remained in solution.
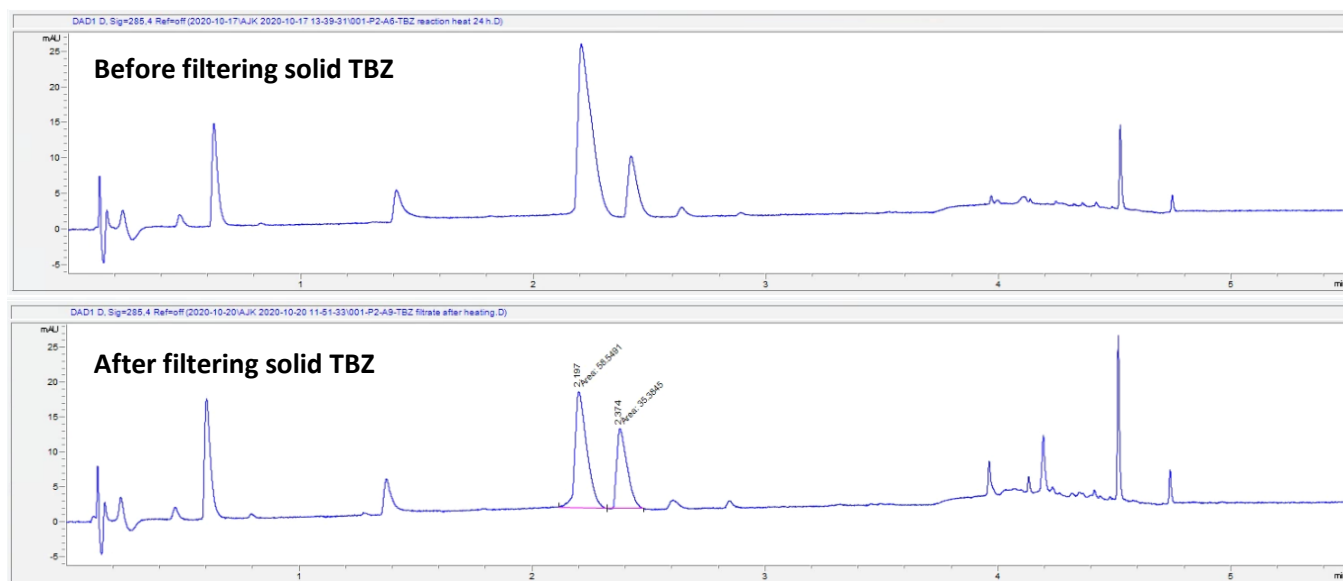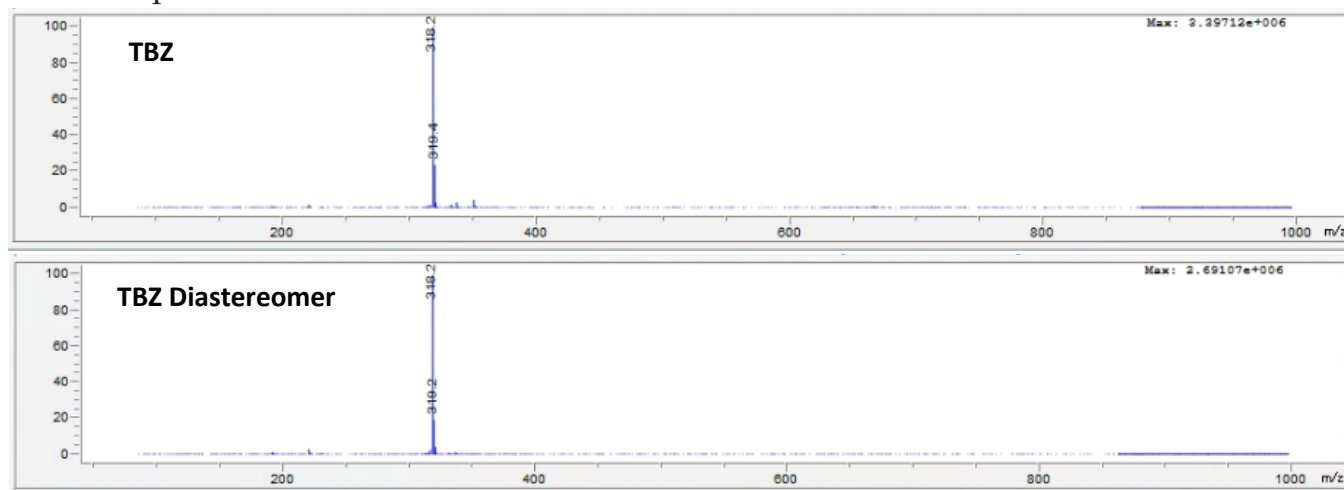
Figure SI 13. HPLC traces (285 nm) of crude TBZ reaction mixture after heating to 60 °C for 4 days (above) and after cooling and filtering off solid TBZ (below) showing significant TBZ diastereomer elution (at 2.37 min) after TBZ (at 2.20 min).
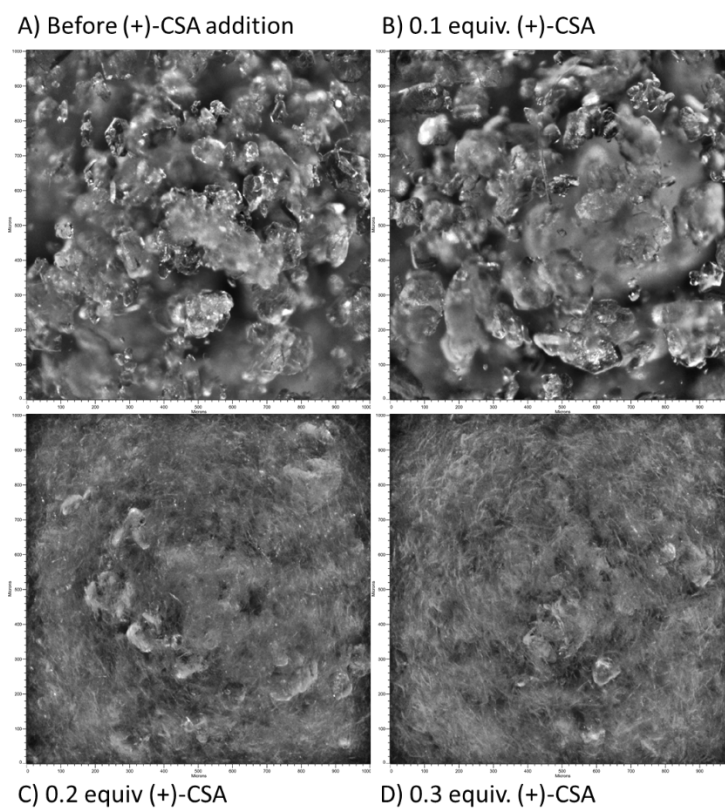
b. UV-Vis Spectra
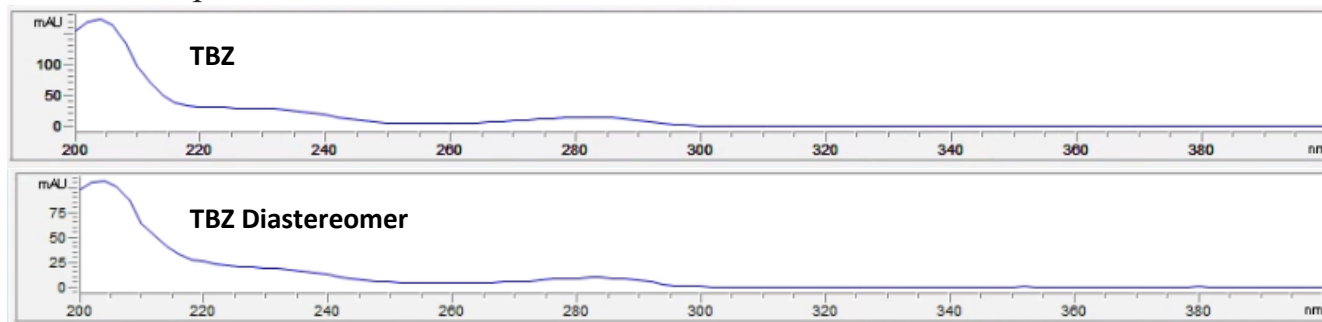
**Figure SI 14.** UV-vis spectra of TBZ (top) and TBZ diastereomer (bottom).

c. Mass Spectra

**Figure SI 15.** MS peaks corresponding to TBZ (top) and TBZ diastereomer (bottom).

d. EasyViewer Images

A) Before (+)-CSA addition
B) 0.1 equiv. (+)-CSA
C) 0.2 equiv (+)-CSA
D) 0.3 equiv. (+)-CSA

Figure SI 16. Images of solid phases during classical resolution, showing difficulty in observing large TBZ solid phase as smaller, needle-like (+)-TBZ·(+)-CSA solids block the probe window

c. Classical Resolution: Entire Experiment
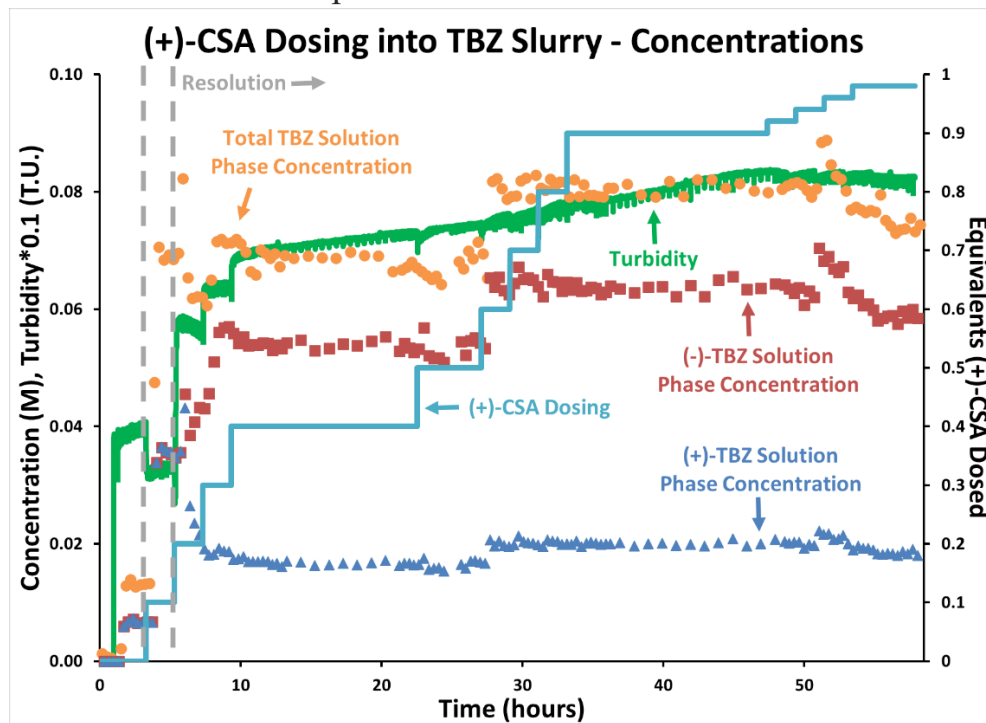
Figure SI 17. Monitoring component concentrations during entire 58.5 hour classical resolution experiment by dosing (+)-CSA solution into saturated TBZ solution (all in 1:1 IPA:water, v/v). Turbidity values were multiplied by a constant (0.1) to be plotted on the same axis as concentration.
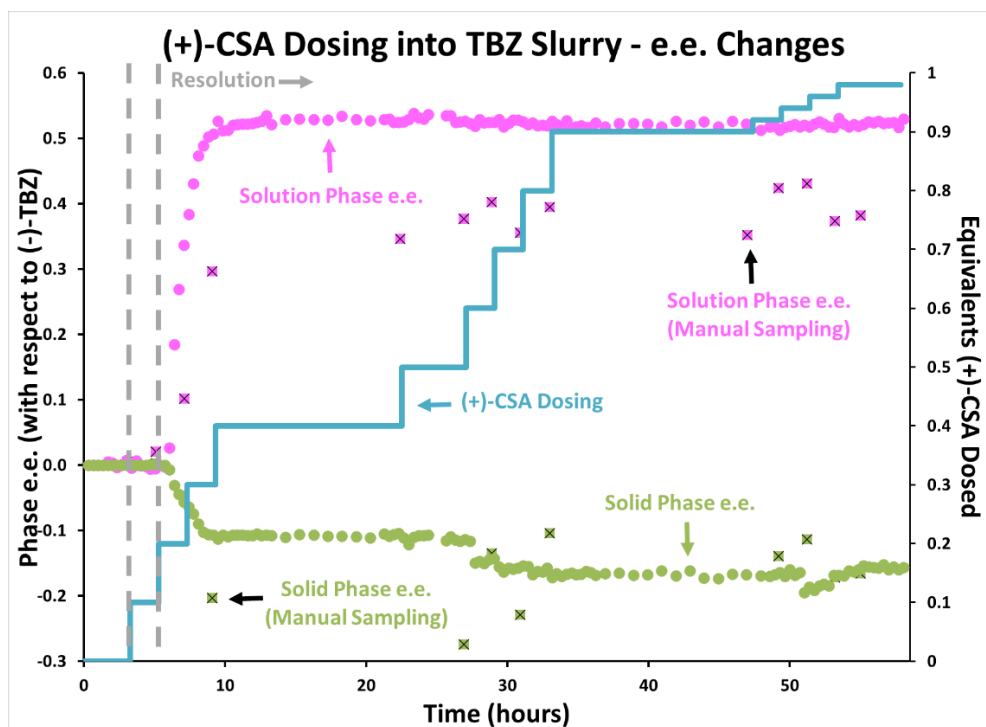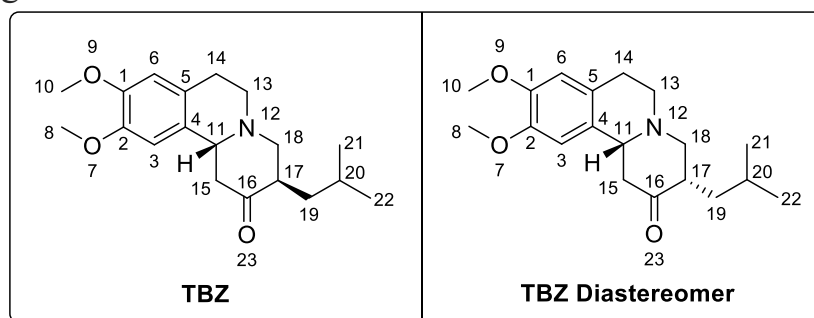

Figure SI 18. Monitoring e.e.'s of phases during entire 58.5 hour classical resolution experiment by dosing (+)-CSA solution into saturated TBZ solution (all in 1:1 IPA:water, v/v), contrasted with manual sampling.

9. NMR Spectra

a. Structural Assignments

Figure SI 19. Structures of TBZ and TBZ diastereomer with atoms numbered (only one enantiomer of each compound is shown).

Atom #	^{1}H		^{13}C	
	TBZ	**Diastereomer**	**TBZ**	**Diastereomer**
1*	---	---	147.9	147.7
2*	---	---	147.6	147.7
3	6.55 s	6.56 s	107.9	107.8
4	---	---	128.5	128.9
5	---	---	126.1	126.6
6	6.62 s	6.62 s	111.5	111.4
8*	3.86 s	3.86 s	56.1	56.1
10*	3.83 s	3.83 s	56.0	56.0
11	3.51 dd J = 11.8, 2.9 Hz	3.44 br d J = 11.5 Hz	62.5	62.2
13	3.19 – 3.05 m 2.64 – 2.49 m	3.07 – 2.93 m 2.58 – 2.49 m	50.7	51.8
14	3.19 – 3.05 m, 2.81 – 2.67 m	3.19 – 3.08 m 2.68 – 2.59 m	29.4	29.4
15	2.90 dd J = 13.6, 3.1 Hz 2.64 – 2.49 m	2.82 ddd J = 14.2, 3.3, 1.5 Hz 2.68 – 2.59 m	47.6	45.4
16	---	---	210.1	212.6
17	2.81 – 2.67 m	2.58 – 2.49 m	47.5	49.2
18	3.29 dd J = 11.5, 6.3 Hz 2.36 t J = 11.6 Hz	3.07 – 2.93 m 2.72 dd J = 11.6, 4.0 Hz	61.5	59.8
19	1.80 ddd J = 13.9, 8.5, 5.5 Hz 1.04 ddd J = 13.6, 7.4, 5.8 Hz	1.85 – 1.73 m 1.60 – 1.46 m	35.1	40.7
20	1.66 ddt J = 12.9, 8.5, 6.5 Hz	1.60 – 1.46 m	25.5	25.9
21*	0.92 appt dd J = 6.6, 4.7 Hz	0.93 d J = 6.2 Hz	23.3	22.8
22*	0.92 appt dd J = 6.6, 4.7 Hz	0.88 d J = 6.3 Hz	22.2	22.4

Table SI 1. Assignment of ^{1}H (400 MHz) and ^{13}C (100 MHz) chemical shifts for TBZ and TBZ diastereomer based on all available spectra. Assignments for TBZ Diastereomer ^{13}C shifts were made based on HMBC as quaternary carbon signals were not visible in the standard ^{13}C spectrum. *Assignments for atoms 1/2, 8/10, and 21/22 are not explicitly assigned and may be interchanged.
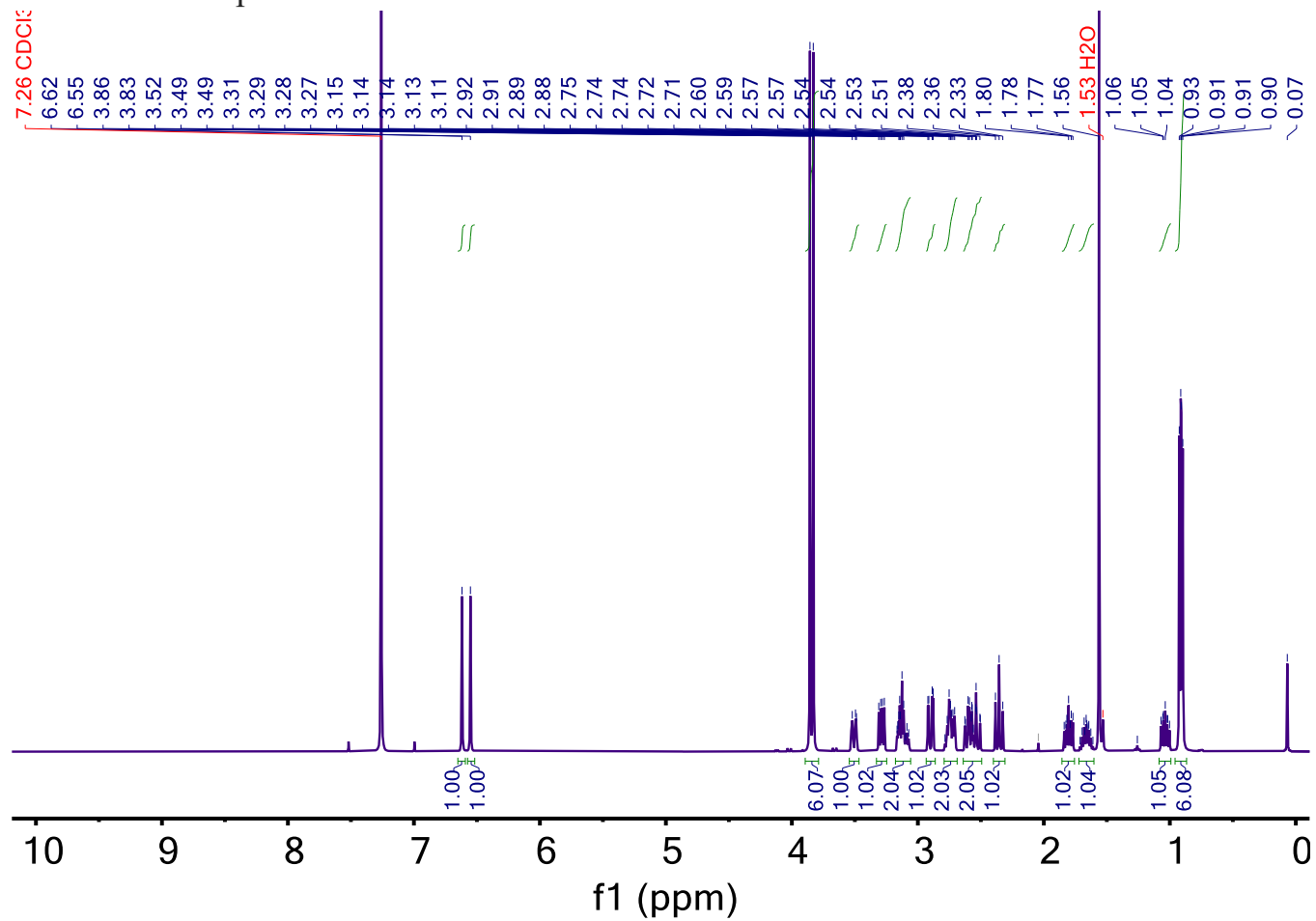
b. TBZ NMR Spectra

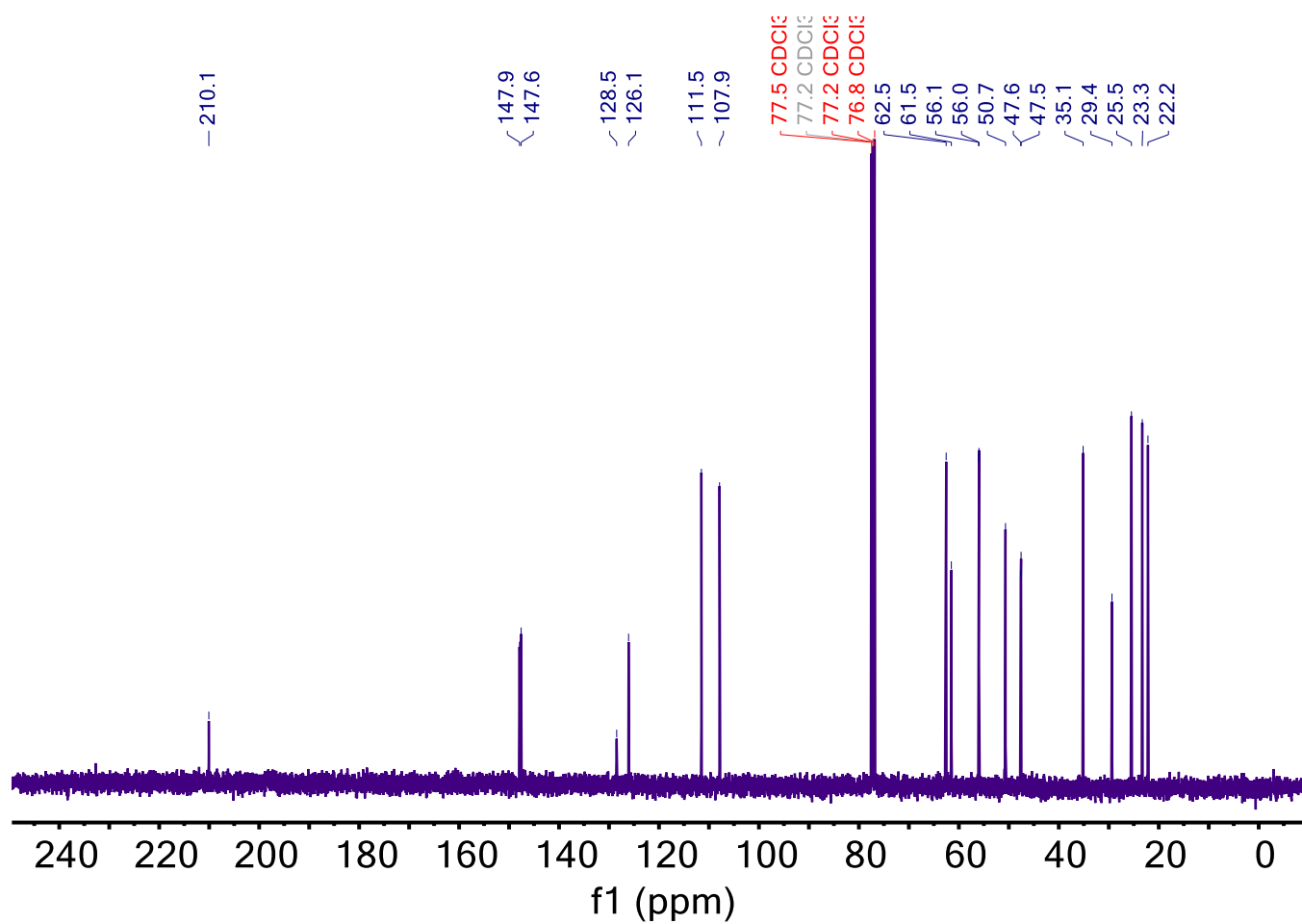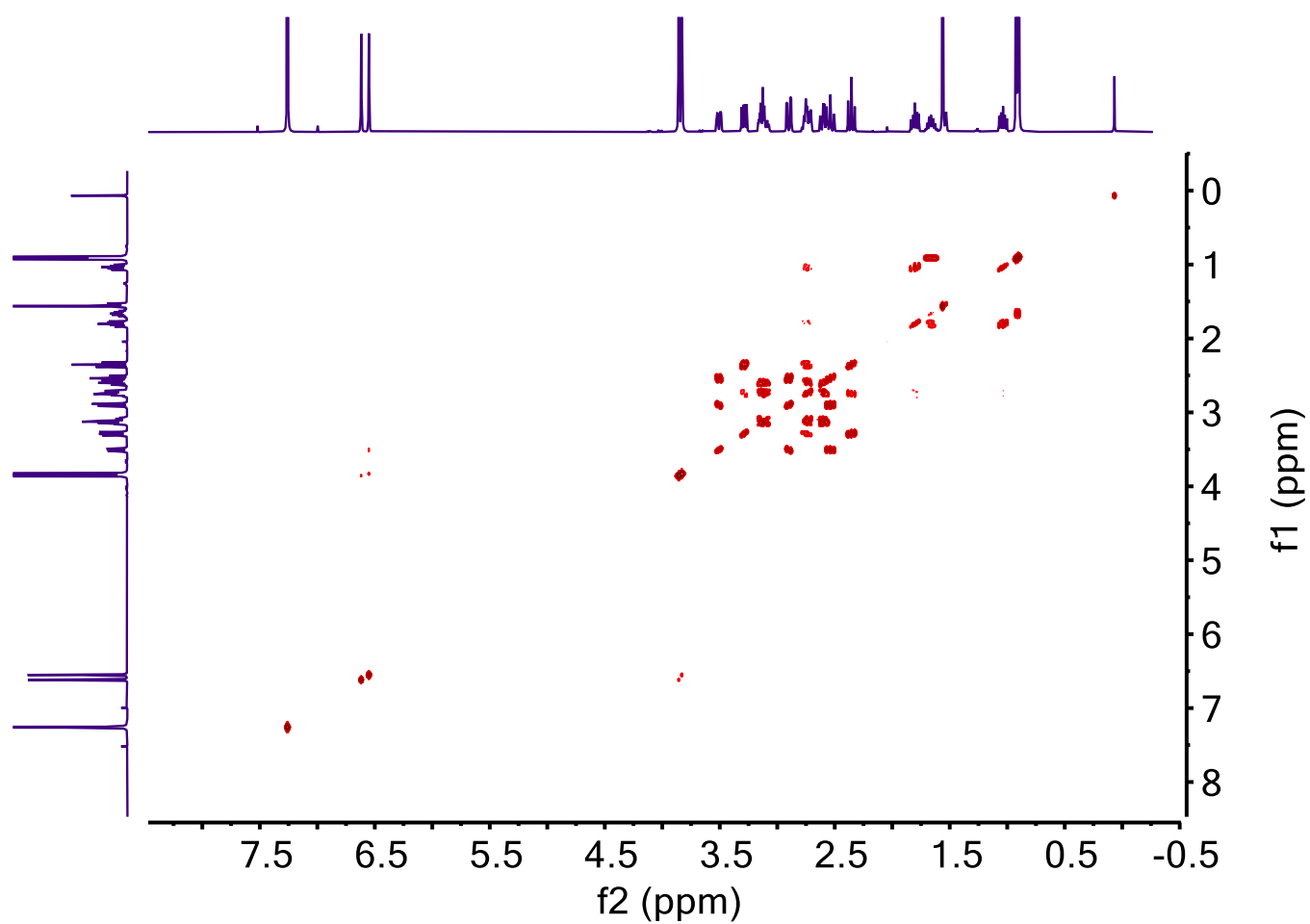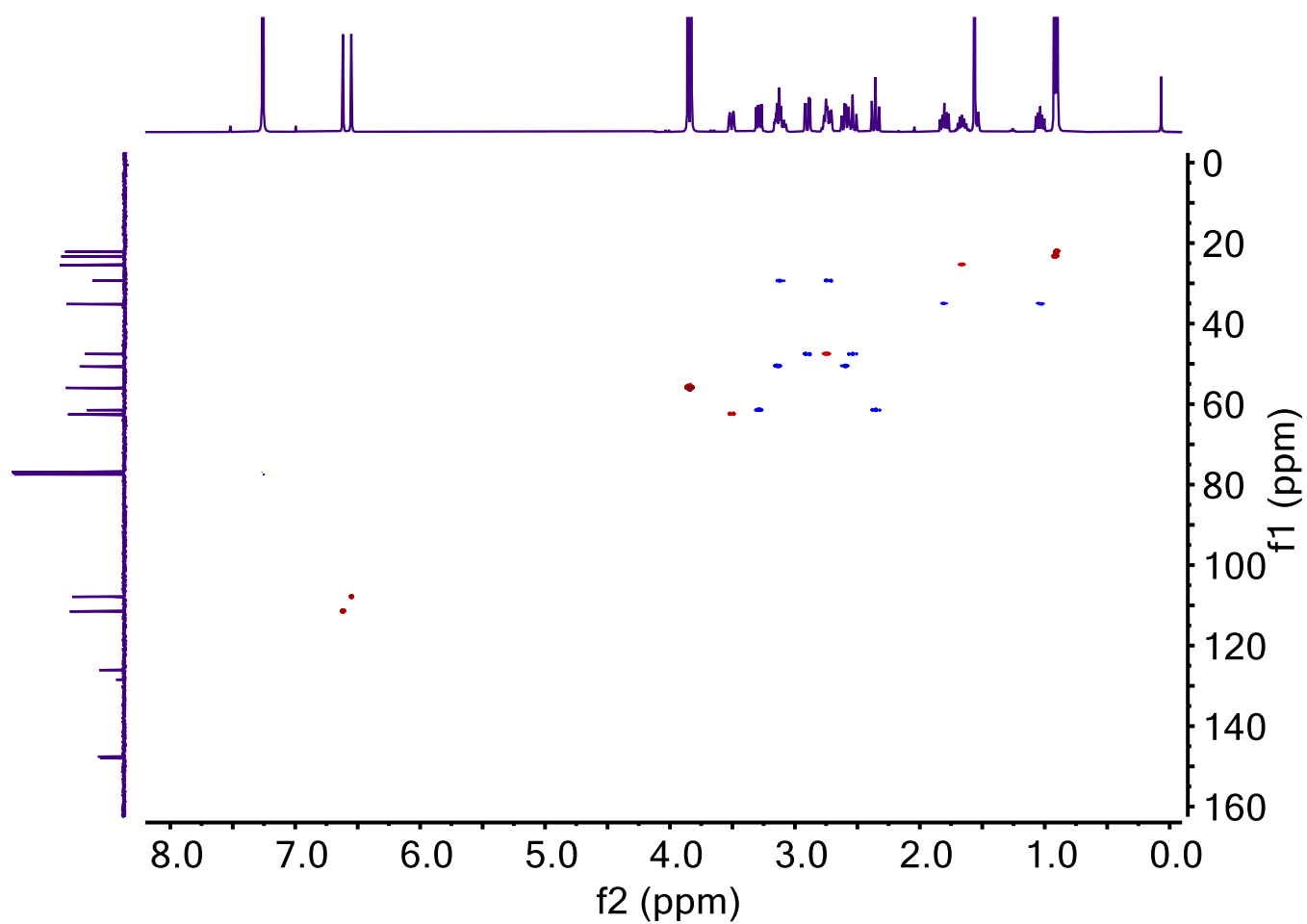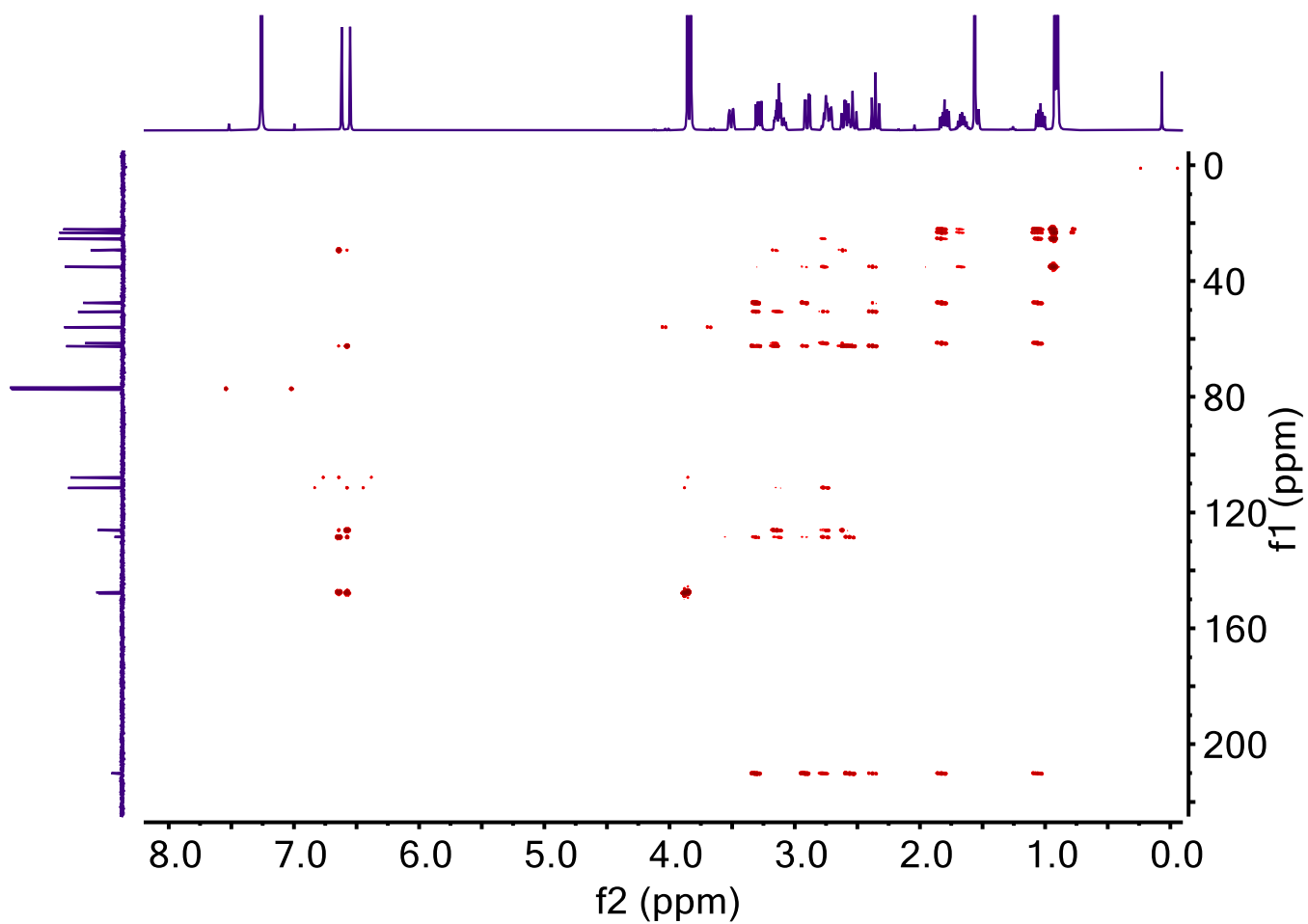**Figure SI 20.** ^{1}H NMR (400 MHz, CDCl$_3$) spectrum of TBZ.

Figure SI 21. ^{13}C NMR (100 MHz, CDCl$_3$) spectrum of TBZ.

Figure SI 22. COSY NMR (400 MHz, CDCl₃) spectrum of TBZ.

Figure SI 23. HSQC NMR (^{1}H: 400 MHz, ^{13}C: 100 MHz, CDCl$_3$) spectrum of TBZ.

Figure SI 24. HMBC NMR (^{1}H: 400 MHz, ^{13}C: 100 MHz, CDCl$_3$) spectrum of TBZ.
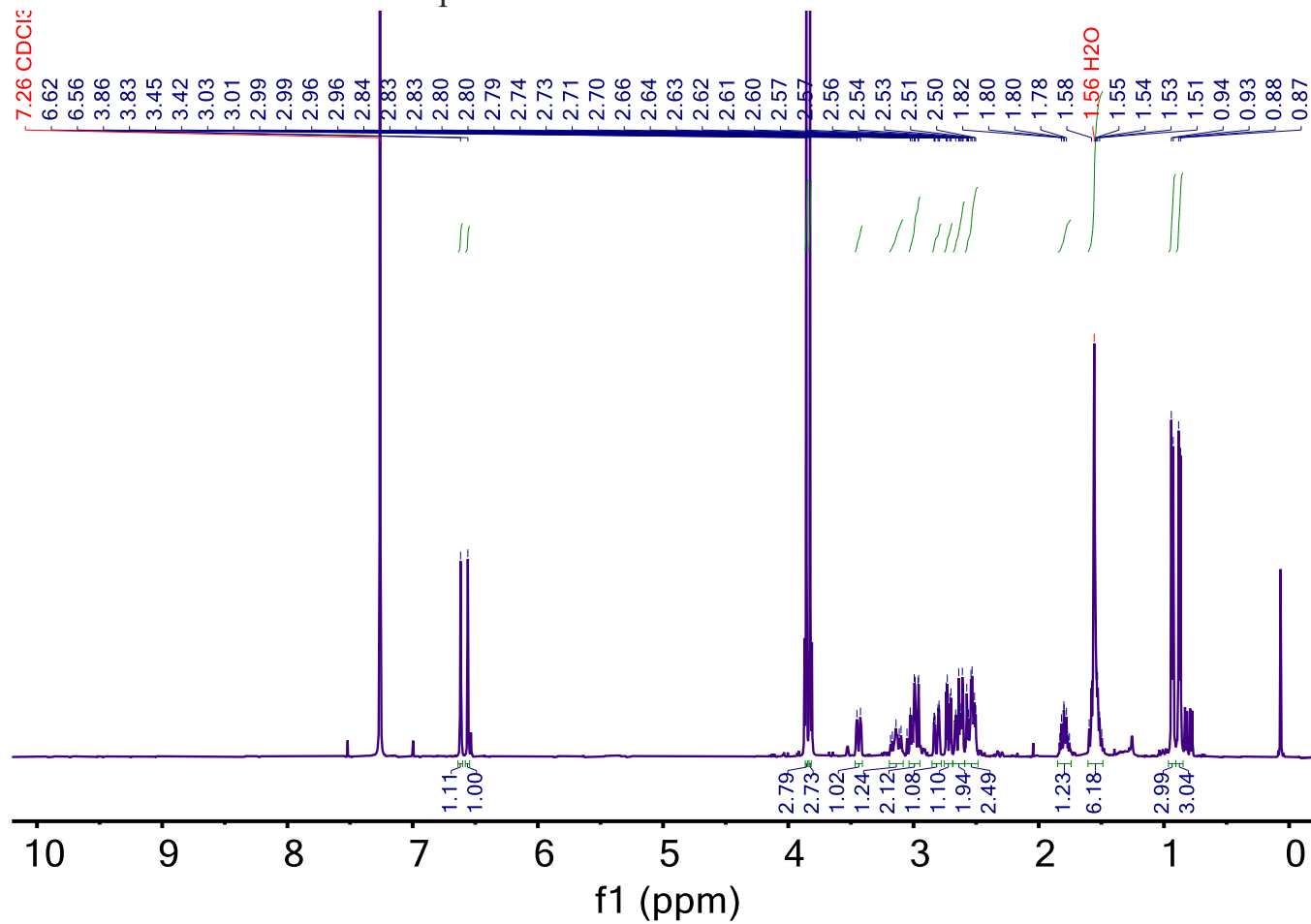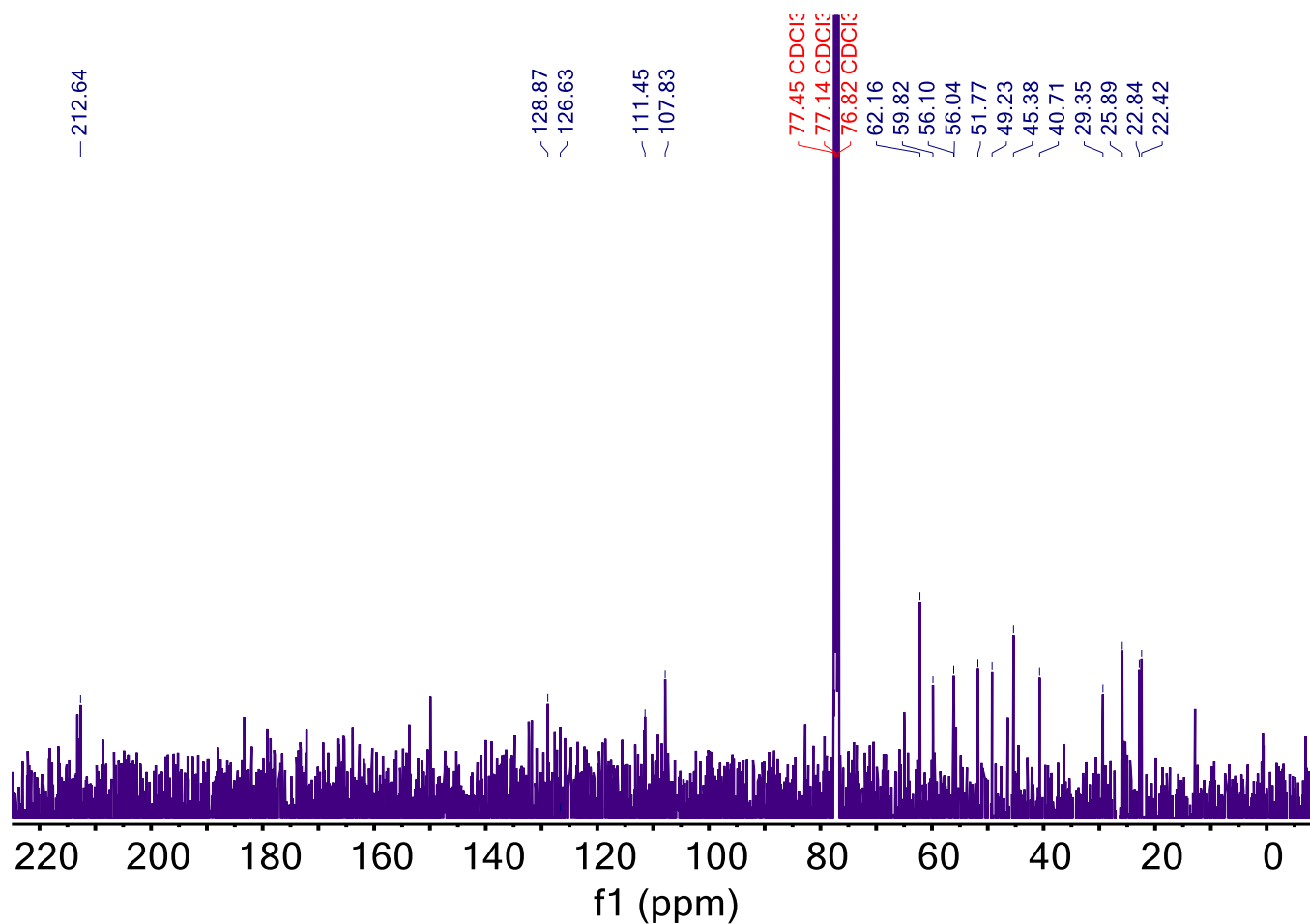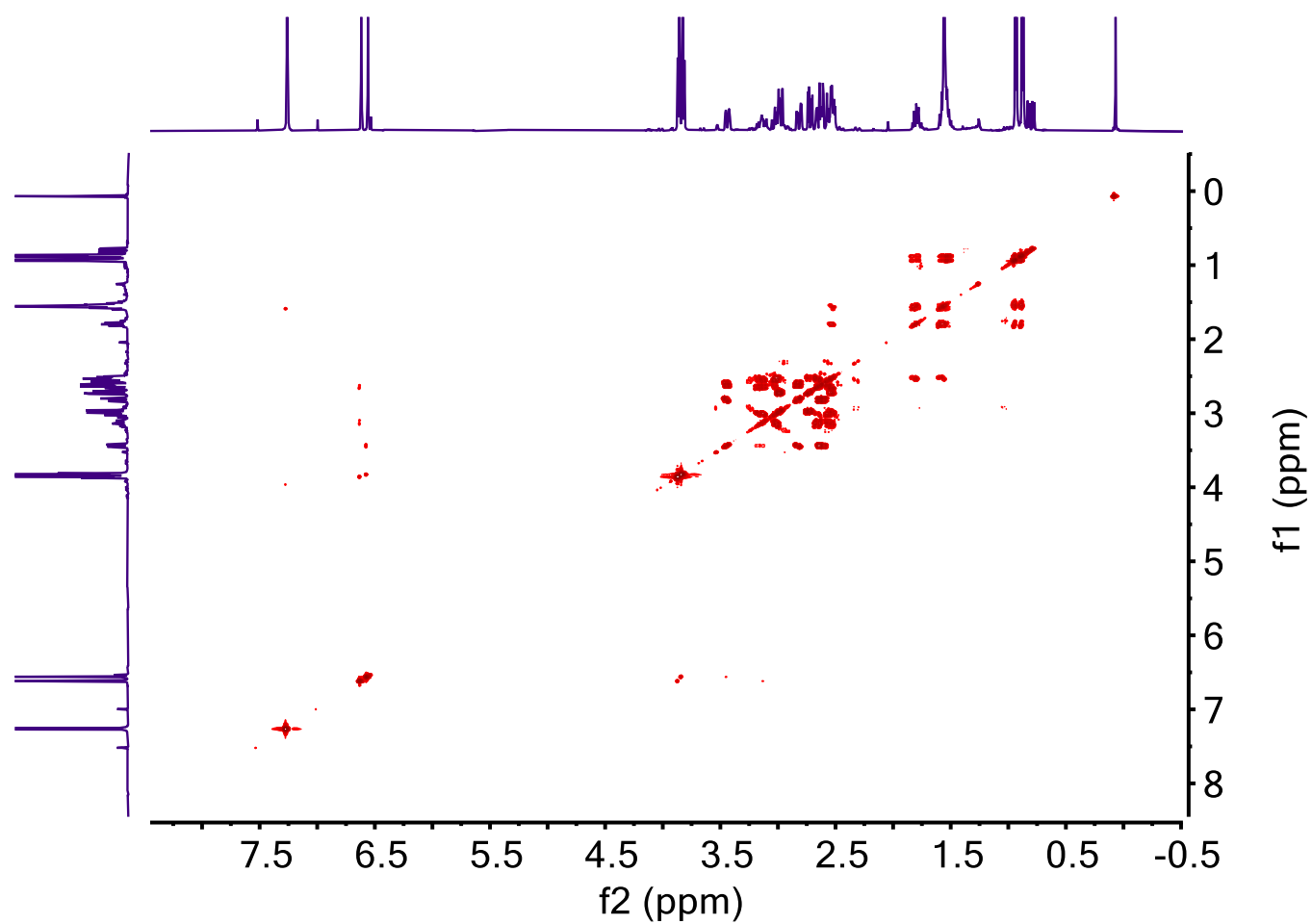
c. TBZ Diastereomer NMR Spectra

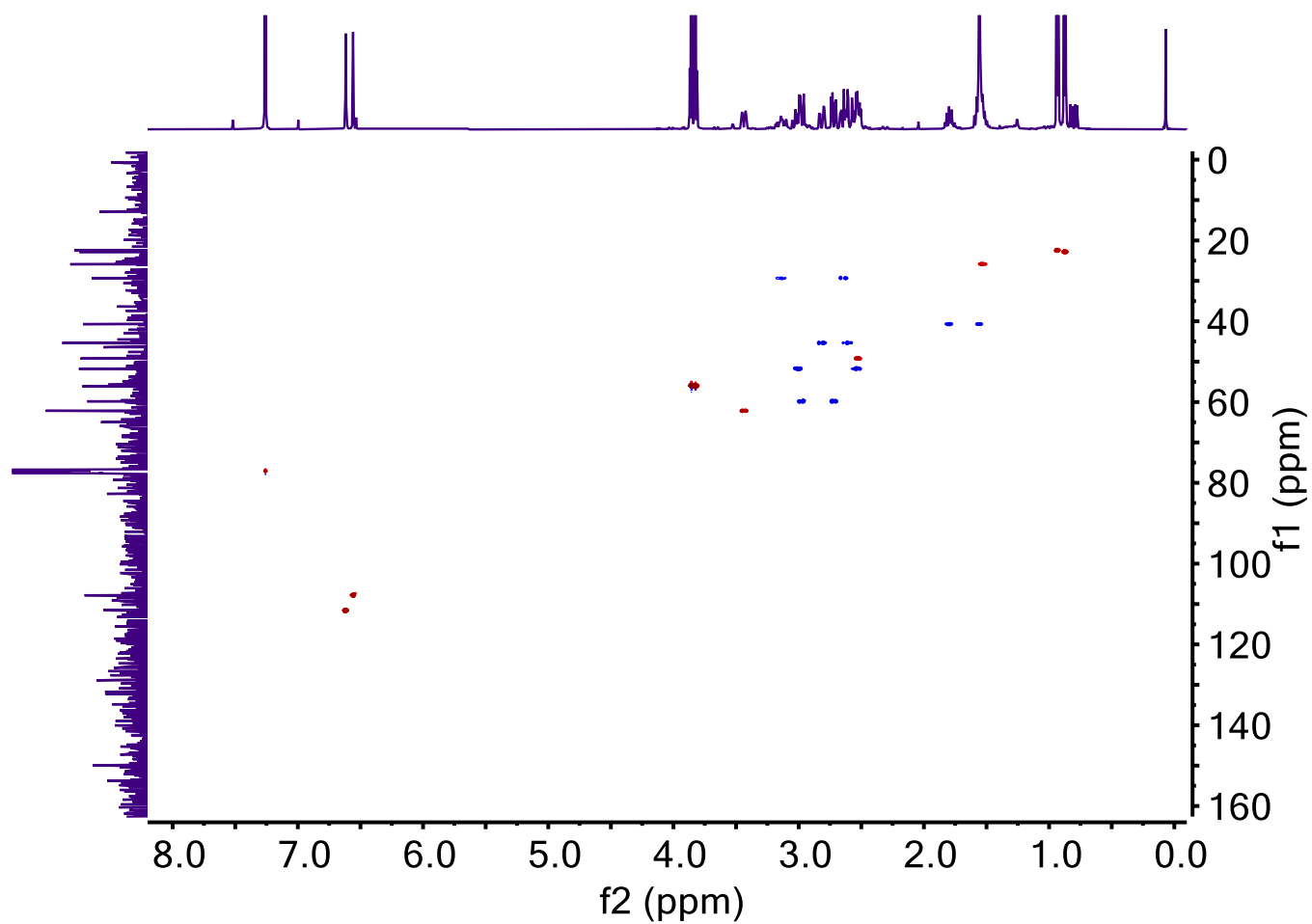**Figure SI 25.** ^{1}H NMR (400 MHz, CDCl$_3$) spectrum of TBZ diastereomer.

Figure SI 26. ^{13}C NMR (100 MHz, CDCl$_3$) spectrum of TBZ diastereomer. HMBC was used in place of this spectrum to assign ^{13}C peaks due to the low concentration. Quaternary signals at 147.7 ppm are not visible amongst the background noise in this spectrum and so are not labeled.
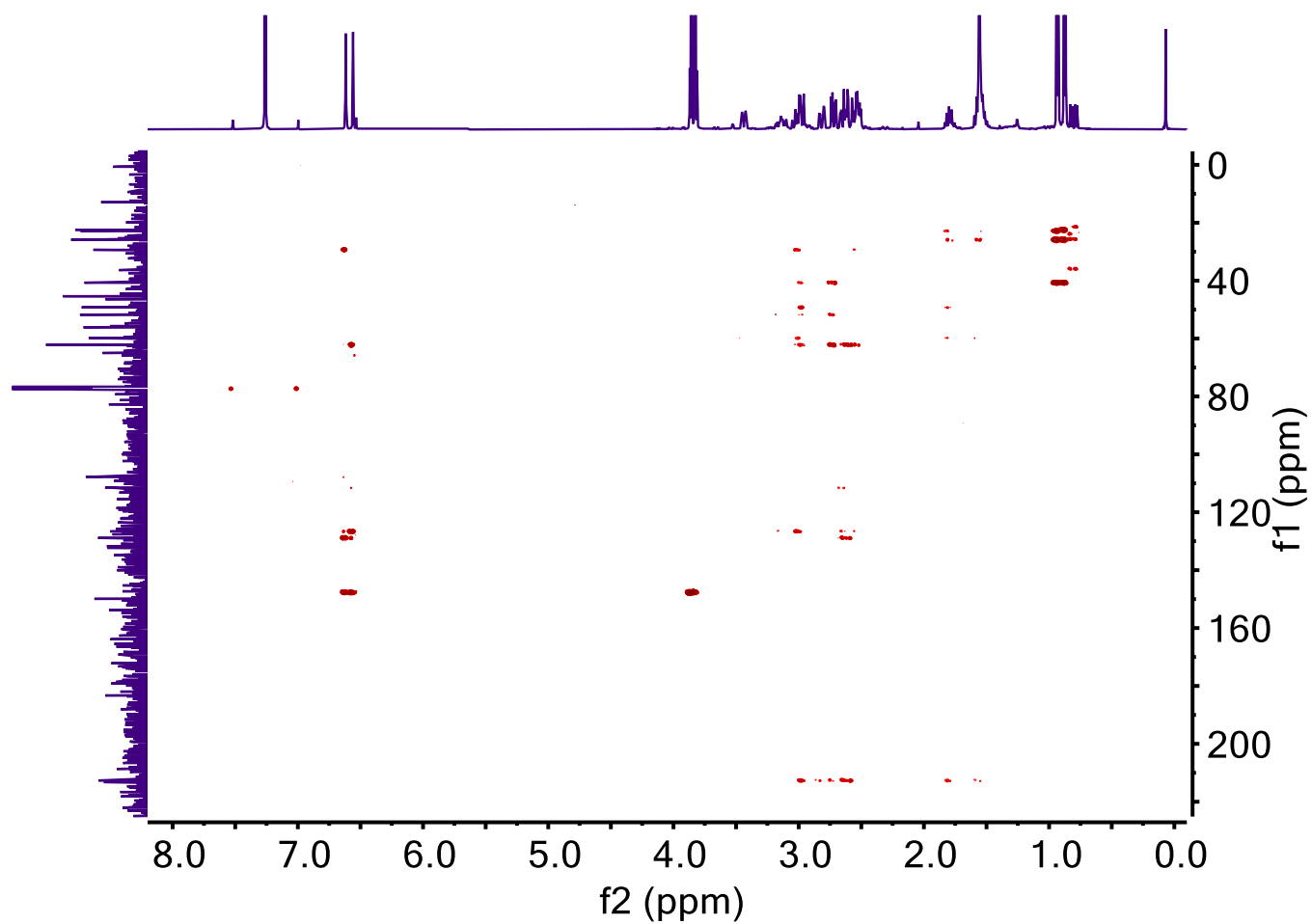
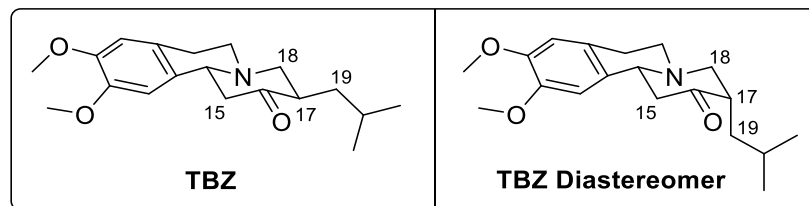**Figure SI 27.** COSY NMR (400 MHz, CDCl₃) spectrum of TBZ diastereomer.

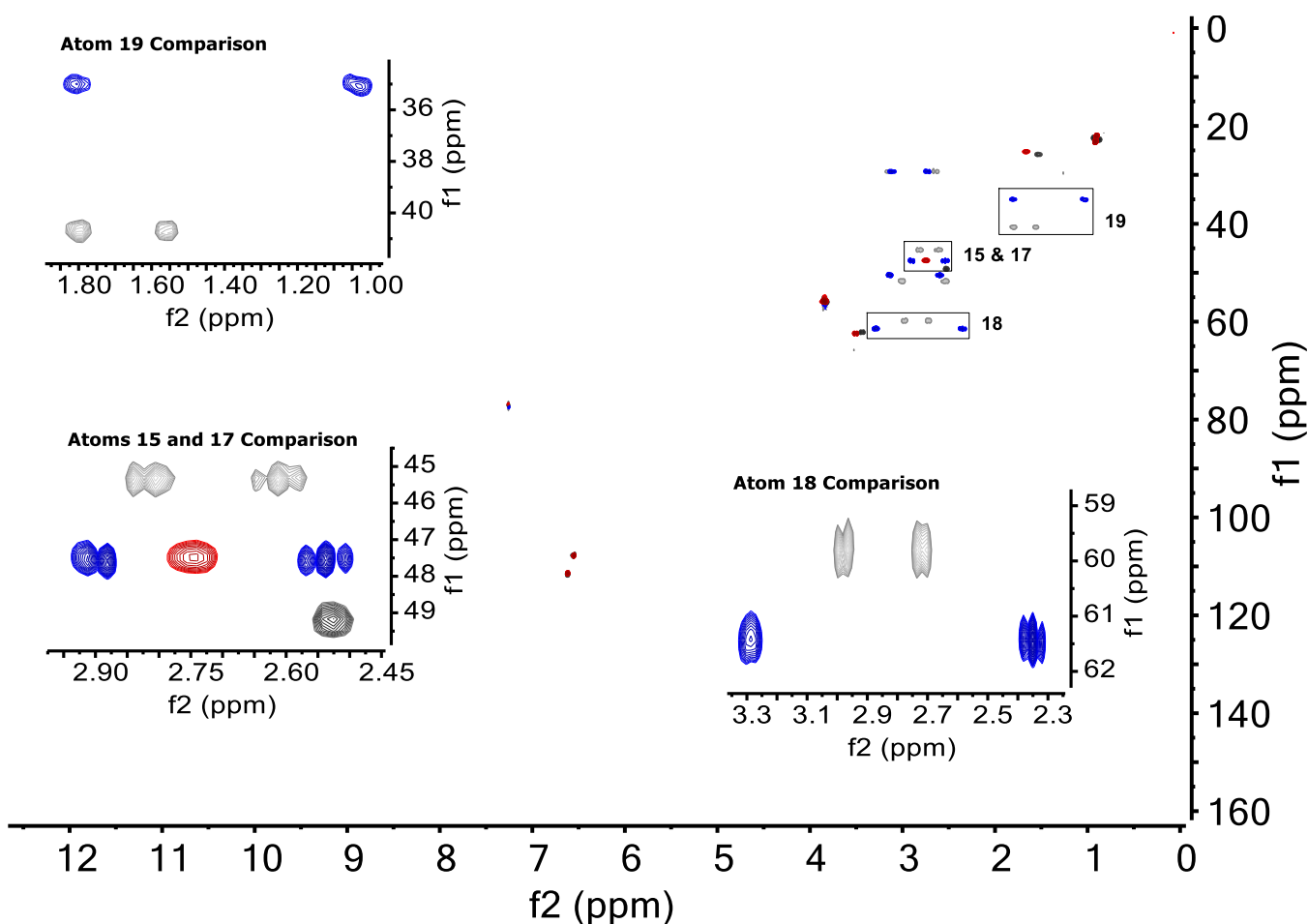**Figure SI 28.** HSQC NMR (^{1}H: 400 MHz, ^{13}C: 100 MHz, CDCl$_3$) spectrum of TBZ diastereomer.

Figure SI 29. HMBC NMR (^{1}H: 400 MHz, ^{13}C: 100 MHz, CDCl$_3$) spectrum of TBZ diastereomer.

d. Diastereomer Identification – HSQC Comparison

Figure SI 30. Proposed geometries of TBZ and TBZ diastereomer (only one enantiomer of each is shown). Atoms with key observable differences in HSQC spectra are labelled.
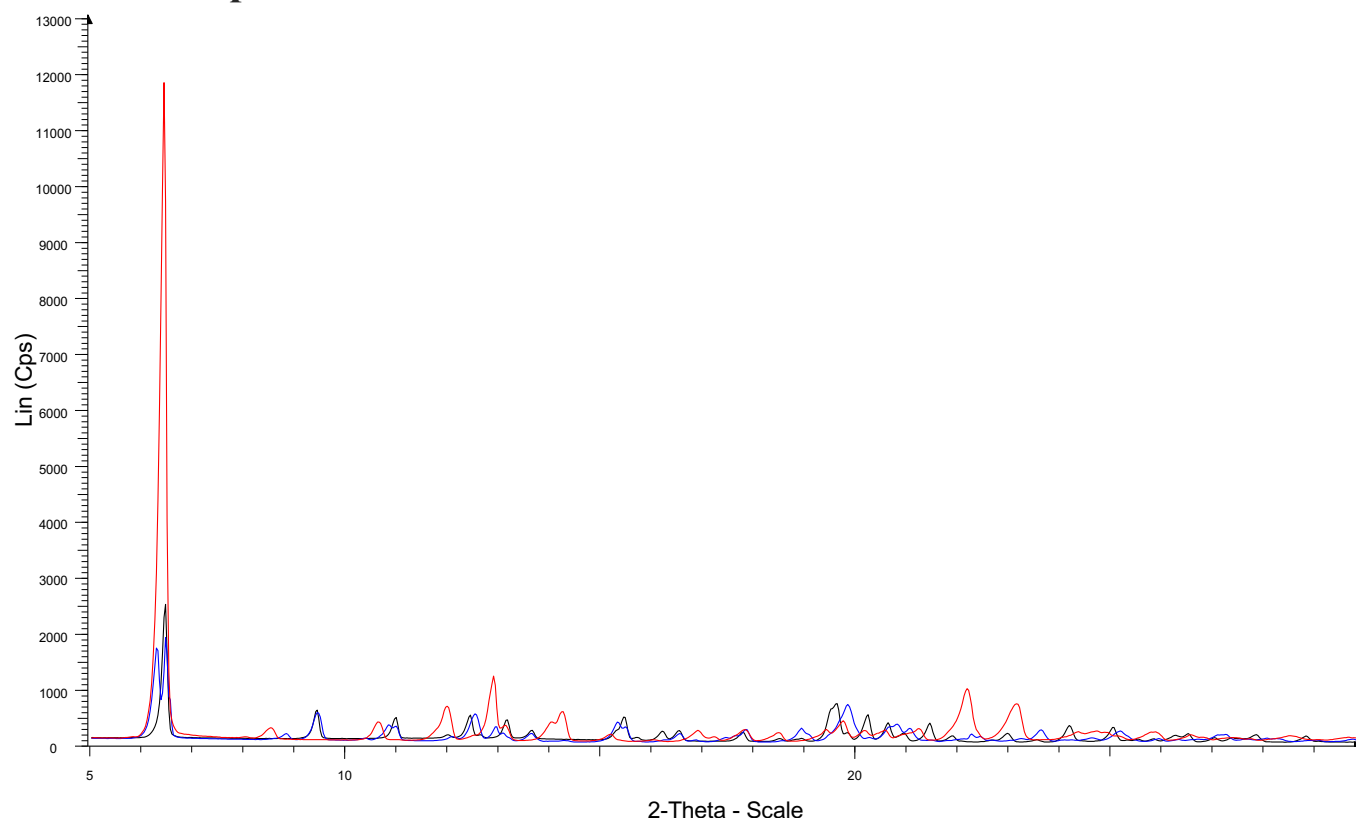

Figure SI 31. HSQC NMR (^{1}H: 400 MHz, ^{13}C: 100 MHz, CDCl$_3$) spectra of TBZ (colour) and TBZ diastereomer (greyscale) with insets comparing shifts of atoms number 15, 17, 18 and 19.

As illustrated in **Figure SI 30**, TBZ and its diastereomer are proposed to differ in the position of the isobutyl group on each of their chair conformations, with it changing from equatorial to axial between TBZ and the diastereomer respectively. This results in observable differences in the ^{1}H and ^{13}C signals at positions 15, 17, 18 and 19 (**Figure SI 31**). Methylenes 15 and 18 (blue) each change by about 2 ppm in the ^{13}C dimension and show significant differences in the shifts of at least one ^{1}H signal due to the presence of the isobutyl group in the equatorial vs. axial position. Similarly, methine 17 (red) changes in both the ^{1}H and ^{13}C dimensions due to this conformational difference, while methylene 19 (blue) on the isobutyl

36

group shows significant differences in both the ^{1}H and ^{13}C dimensions due to the varying chemical natures of its equatorial vs. axial environments in TBZ and the diastereomer respectively. This data is therefore consistent with the expected conformational change between TBZ and its diastereomer, suggesting that the diastereomer was in fact isolated.

10. PXRD Spectra

File: AJK-2-012.raw - Start: 5.000 ° - End: 59.999 ° - Step: 0.030 ° - Step time: 84. s - Anode: Cu - WL1: 1.5406 - WL2: 1.54439 - kA2 Ratio: 0.5 - Generator kV: 40 kV - Generator mA: 40 mA - Creation: Operations: Import
File: AJK-2-041.raw - Start: 5.000 ° - End: 59.999 ° - Step: 0.030 ° - Step time: 84. s - Anode: Cu - WL1: 1.5406 - WL2: 1.54439 - kA2 Ratio: 0.5 - Generator kV: 40 kV - Generator mA: 40 mA - Creation: Operations: Import
File: AJK-2-063.raw - Start: 5.000 ° - End: 59.999 ° - Step: 0.030 ° - Step time: 84. s - Anode: Cu - WL1: 1.5406 - WL2: 1.54439 - kA2 Ratio: 0.5 - Generator kV: 40 kV - Generator mA: 40 mA - Creation: Operations: Import

Figure S. 32 PXRD spectra of isolated solids: (+)-TBZ·(+)-CSA (black), (±)-TBZ (red), solids from (+)-CSA dosing experiment (blue)

PXRD of solids obtained from the (+)-CSA dosing experiment (blue) is shown overlaid with PXRD of solid (±)-TBZ (red) and (+)-TBZ·(+)-CSA (black). Similar peaks between the black and blue traces suggest that the dosing experiment solid phase is primarily composed of (+)-TBZ·(+)-CSA, but similarities with the red trace suggests (±)-TBZ is also present.

11. References

1. Z. Yao, X. Wei, X. Wu, J. L. Katz, T. Kopajtic, N. H. Greig, H. Sun, *Eur. J. Med. Chem.* **2011**, *46* (5), 1841–1849.
2. J.-G. Park, S.-H. Lee, J.-S. Ryu, Y.-K. Hong, T.-G. Kim, A. A. Busnaina, *J. Electrochem. Soc.* **2006**, *153* (9), G811–G814.